CONDITIONS OF FORMATION OF THE IRON-BEARING SKARNS AT LONE MOUNTAIN, LINCOLN COUNTY, NEW MEXICO

by

David W. Schnake

Submitted in Partial Fulfillment
of the Requirements of the Degree of
Master of Science in Geology

New Mexico Institute of Mining and Technology

Socorro, New Mexico

August, 1977

TABLE OF CONTENTS

LIST OF FIGURES

LIST OF PLATES

LIST OF TABLES

ABSTRACT

The core of Lone Mountain consists of a Tertiary quartz monzonite stock which is shielded by steeply dipping units of the San Andres Formation. Evidence was found which suggests that the stock originally had a larger K-feldspar component which was later albitized by hydrothermal action. Both the stock and the sedimentary rocks are cut by several large quartz monzonite dikes. The southeastern section of the stock is overlain unconformably by a Tertiary volcanic agglomerate.

Contact metamorphism is limited primarily to roof pendants of San Andres limestone, gypsum, and quartzite. The alteration is most extensive at the intersection of the dikes with the stock. The dominant silicate skarn mineral is diopside with lesser amounts of phlogopite, albite, and tremolite. The major iron mineral in most skarns is magnetite with the exception of the Yellow Jacket skarn in which it is hematite.

The skarn was determined to have formed at approximately 250°C and 140 bars. Through the application of the thermodynamic properties of the skarn minerals at the above temperature and pressure, it was found that the skarns are the result of the interaction of meteoric ground waters with the host rocks as they migrated towards the sedimentary-igneous contact from the surrounding sedimentary rocks. Deposition of the iron oxides was initiated by an increasing pH; a result of the dissolution of calcite at the depositional site.

The Ca-Mg silicates were deposited in host rocks with free SiO_2, namely the quartz monzonite and quartzite. Mass transfer calculations indicate that the SiO_2 component of the silicate skarn minerals was furnished by the host rock while the Ca and Mg were introduced by

hydrothermal solutions.

Further evidence is presented which suggests that the location and size of the iron deposits may be to some degree a function of the presence of gypsum units in the San Andres Formation by helping to channel ground water flow into the high temperature depositional areas.

ACKNOWLEDGEMENTS

I wish to express my deep appreciation of the many hours of instruction and guidance offered by my advisor, Dr. R.E. Beane, during the compilation of this manuscript. His eagerness to not only teach but to have his students learn is an all too rare quality among educators today. Acknowledgements are also due to the other thesis committee members, Professors C.T. Smith and A.J. Budding for their helpful suggestions and criticisms.

I would also like to thank the Geoscience Department of the New Mexico Institute of Mining and Technology and the New Mexico Geological Society for their financial assistance.

A special thanks goes to Carol Schnake, for without her I'm certain none of this would ever have come to pass.

INTRODUCTION

Lone Mountain is located approximately 10 miles north of Carrizozo in Lincoln County, New Mexico, (Fig. 1). Sheridan (1947) presented the first published account of the geology and ore deposits of Lone Mountain; however, the main intent of his report was an economic evaluation of the active iron mines of Lincoln County, and therefore contained only a very general description of the geology. Later investigations by Kelley (1949), Griswold (1959), and Walker and Osterwald (1956) offered only brief reviews of the geologic relationships.

The geology of Lone Mountain was first mapped by Smith and Budding (1959) on a scale of 1:62000 and later described in more detail by Smith (1964). Butler (1964) described the petrology of the Lone Mountain laccolith and analyzed the magnetite ores for titanium content. To date, however, there have been no attempts to accurately determine the mineralogy, paragenesis, or origin of the Lone Mountain skarns and associated iron deposits.

The purpose of this study was to establish the thermochemical conditions prevalent during the formation of the iron-bearing skarns at Lone Mountain. The probable origin and composition of the mineralizing solutions is determined on the basis of information gained from a detailed investigation of the geology, petrology, and mineralogy of the Lone Mountain intrusives and associated contact metamorphic zones.

The study area covers approximately 9 square miles of R. 11 E., T. 6 S., with the perimeter and most of the larger mines readily accessible via dirt roads leading from the ghost towns of Coyote and White Oaks. The roads are generally passable year round with the

Figure 1. Location map of New Mexico showing the location of Lincoln County and Lone Mountain.

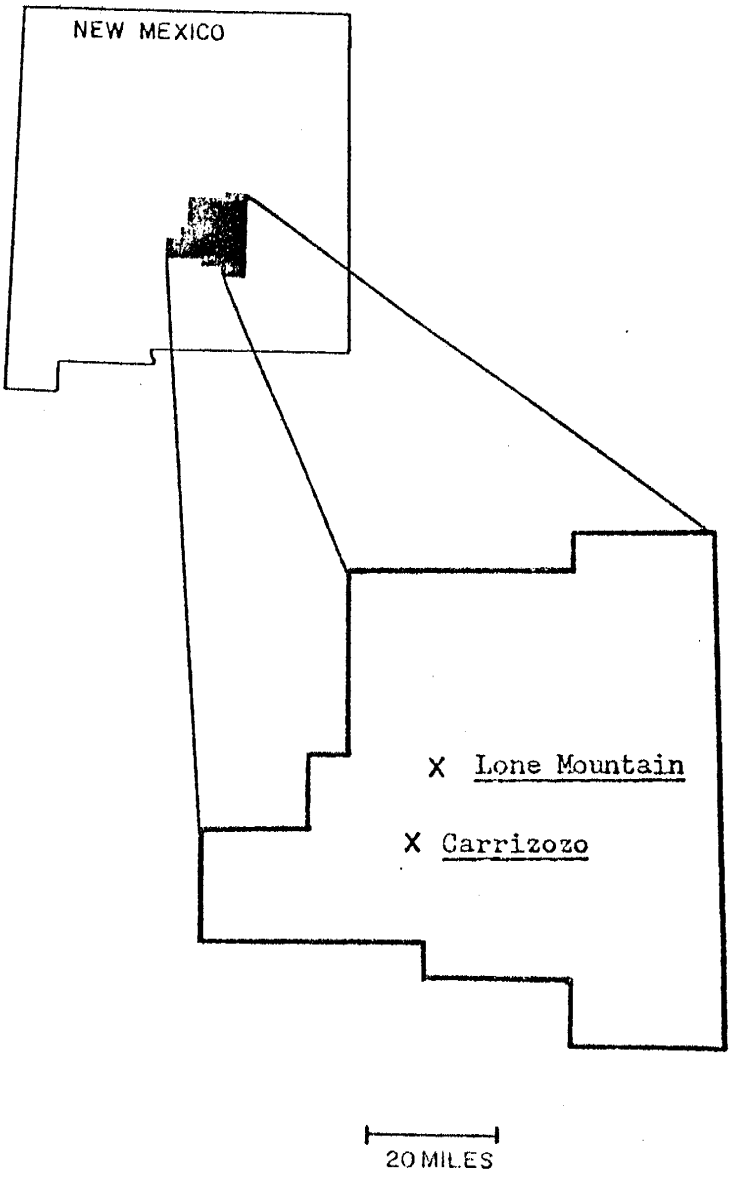
NEW MEXICO
X Lone Mountain
X Carrizozo
20 MILES

exception of those roads leading to the northeast quadrant of the area which may become deeply eroded during heavy rains.

The geology of the Lone Mountain area was mapped on a scale of 1:12000 using an enlarged copy of the Little Black Peak Quandrangle topographic sheet as a base map. Samples of the stock, dikes, and skarns were collected during the mapping for later use in petrographic chemical, and X-ray diffraction analysis. Thirty-eight thin sections were prepared for petrographic analysis, and twenty-two silicate rock samples were analyzed for SiO_2, Al_2O_3, FeO, MgO, CaO, Na_2O, K_2O, and MnO by flame atomic absorption spectroscopy. In addition, three samples of limestone were analyzed for SiO_2, CaO, MgO, MnO, CO_2, and H_2O. Mineral identification was by X-ray diffraction methods and thin section examination. Bulk samples were analyzed on the diffractometer while very limited or small crystals were determined with a Debye-Scherrer camera.

INTRUSIVE ROCKS

Lone Mountain is located at the approximate intersection of two major structural features: the Mescalero Arch and the Capitan Lineament (Fig. 2). The Mescalero Arch extends from the Sacremento uplift northeasterly to the southern flank of the Capitan intrusive. North of this intrusive the arch has been shifted approximately 15 miles to the west where it continues northward toward Corona; Lone Mountain rests on the downfaulted western limb of the arch (Fig. 2). An east-west alignment of igneous features extending from west Texas to western New Mexico is often referred to as the Capitan Lineament. Kelley and Thompson (1964) suggest the lineament is a major hinge zone, possibly active since Precambrian time, but they also postulate that the east-west alignment of intrusives may be the result of the hinge zone being in part a fracture zone.

The Lone Mountain intrusive is one of at least ten Tertiary stocks and laccoliths occurring in the region between Corona and Ruidoso (Fig. 2). Numerous small domes and doubly plunging anticlines in the region suggest the presence of additional covered stocks. On the basis of observing stocks overlain by volcanics and stocks cutting the volcanics, it is evident that there were at least three stages of igneous activity during Tertiary time. However, the lack of isotope age dates and scarce field relationships prevent the determination of the order in which the numerous plutons were intruded.

The intrusive rocks exposed in the vicinity of Lone Mountain consist of a laccolithic pluton of about 5 square miles in outcrop area and a number of small dikes and sills. These dikes and sills cut both the

Figure 2. Major structural zones and structural features in the Lone Mountain area, L = laccolith; S = stock; Q = quaternary basalt flow.

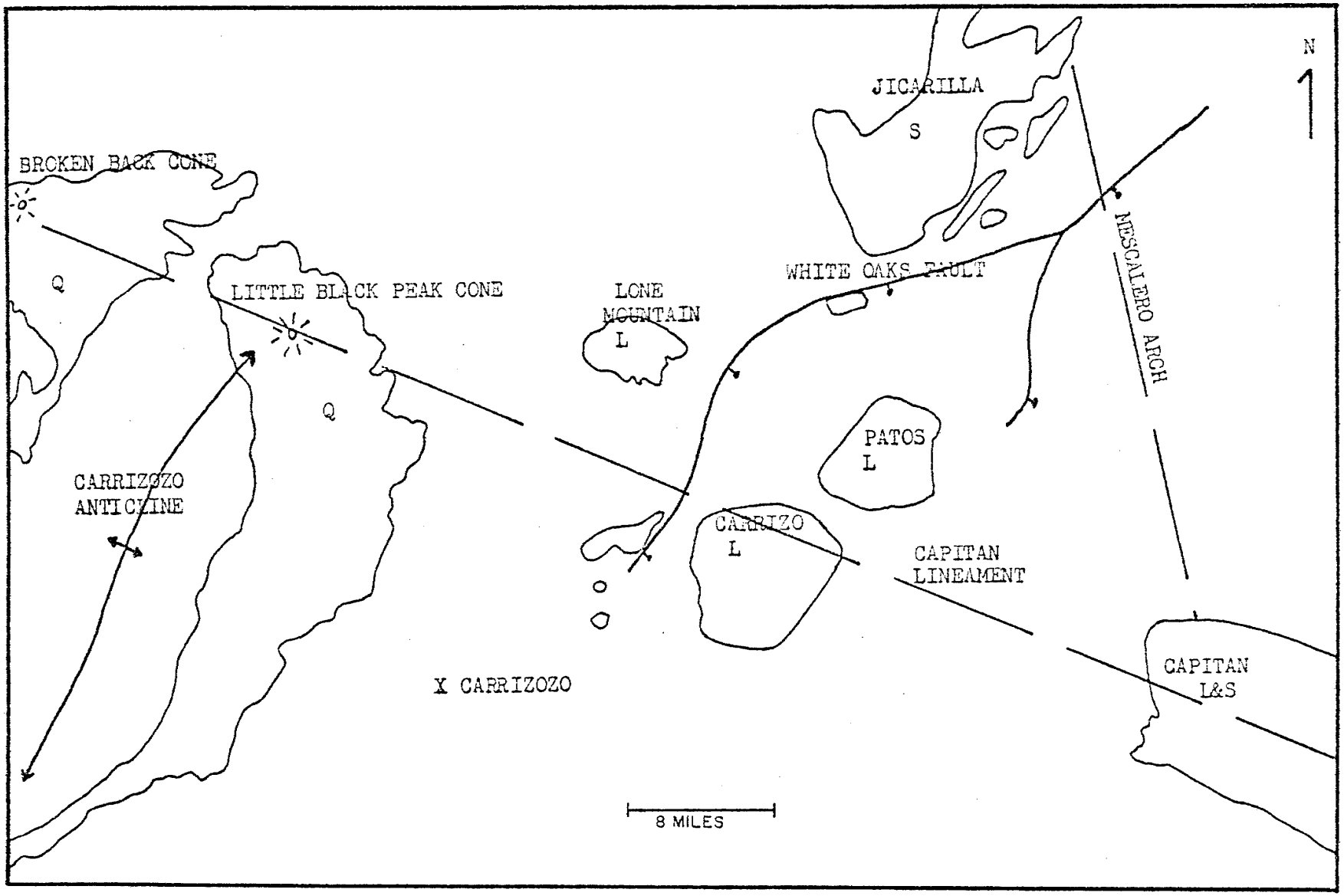
N
JICARILLA
S
BROKEN BACK CONE
Q
LITTLE BLACK PEAK CONE
Q
LONE
MOUNTAIN
L
WHITE OAKS FAULT
MESCALERO ARCH
PATOS
L
CARRIZOZO
ANTICLINE
CARRIZO
L
CAPITAN
LINEAMENT
CAPITAN
L&S
X CARRIZOZO
8 MILES

pluton and the surrounding Paleozoic sedimentary rocks (Plate 1).

Viewed locally the Lone Mountain intrusive is laccolithic in that the igneous-sedimentary contact approximately parallels the sedimentary bedding where it is steeply folded. Regionally, however, the contact angle greatly exceeds the general dip of the bedding and therefore may also be correctly defined as a stock. During the early stages of intrusion, lateral movement of the magma was enhanced by the presence of incompetent gypsum beds within the San Andres Formation which were easily folded and compressed. This method of intrusion is well documented along the Jones dike 25 miles to the west where gypsum within the Yeso Formation served as passage ways for sills which in places extend over 1000 feet from the dike (Kelley and Thompson, 1964). At Lone Mountain the force required for lateral movement eventually exceeded the force required for vertical movement and the magma domed and possibly cut through the overlying sediments.

Very limited outcroppings of lamprophyre(?) dikes occur in the southeastern portion of the study area. These dikes are of an obscure affinity but are possibly related to the lamprophyre dikes of the White Oaks mining district, 2½ miles to the east (Smith, 1964). Because the lamprophyre dikes offer limited exposures and show no relationship to the Lone Mountain mineralization, they will not be discussed to any further extent below.

Lone Mountain Laccolith

The Lone Mountain laccolith is very uniform in texture considering its large size. The rock is predominately an aphanitic porphyry, although some samples from the center of the pluton exhibit a phaneritic equigranular texture. Most of the phenocrysts consist of euhedral

antiperthite or untwinned albite; these crystals typically have lightly corroded edges. The K-feldspar of the antiperthite, which generally makes up less than ten percent of a phenocryst, occurs as thin laminae or blebs in the albite host, often giving the phenocrysts a cloudy appearance at low magnification, x25. Two samples from the northeast portion of the pluton also contained phenocrysts of deeply embayed subhedral quartz. The aphanitic groundmass is comprised of anhedral to subhedral crystals of microcline, plagioclase, quartz, and mafic minerals. The microcline displays characteristic plaid extinction and shows no signs of albite exsolution. Twinned plagioclase laths are rare, but when present they are usually rimmed by sericite (Fig. 3). Quartz is always anhedral and occassionally may completely enclose crystals of feldspar.

Mafic minerals, which rarely constitute more than five percent of the rock, consist of biotite (with slight chloritization), diopside, magnetite, and sphene. Figure 4 indicates the spatial distribution of mafic minerals within the stock as determined from 15 thin sections. On the basis of so few sample locations a definite spatial zoning cannot be established but generally it would appear that the biotite is restricted to the central portion of the intrusive, surrounded peripherally by rocks containing diopside; from thin sections it is apparent that the diopside was formed at the expense of biotite.

Modal analysis of the laccolith samples is impractical because of the porphyritic texture and antiperthite. Therefore whole-rock major element chemical analyse were performed on a representative set of eight samples (Table 1), and normative mineral contents of the rocks were calculated using linear regression analysis to distribute the elements

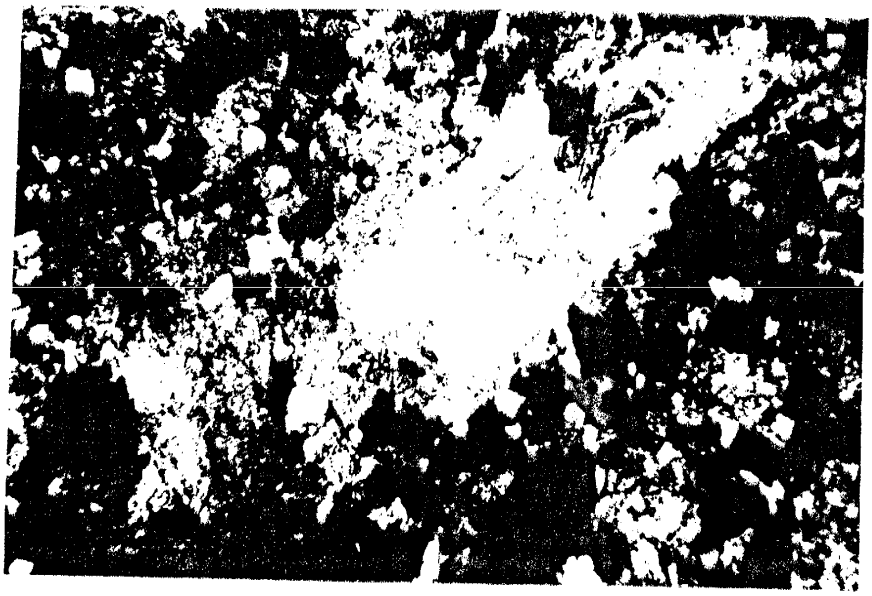

Figure 3. Photomicrograph of a sample from the laccolith showing a lath of plagioclase rimmed by sericite, x-nicols, X100.

Figure 4. Mafic mineralogy of the Lone Mountain Laccolith, (stippled area). B - biotite, C - chlorite, D - diopside, M - magnetite, S - sphene

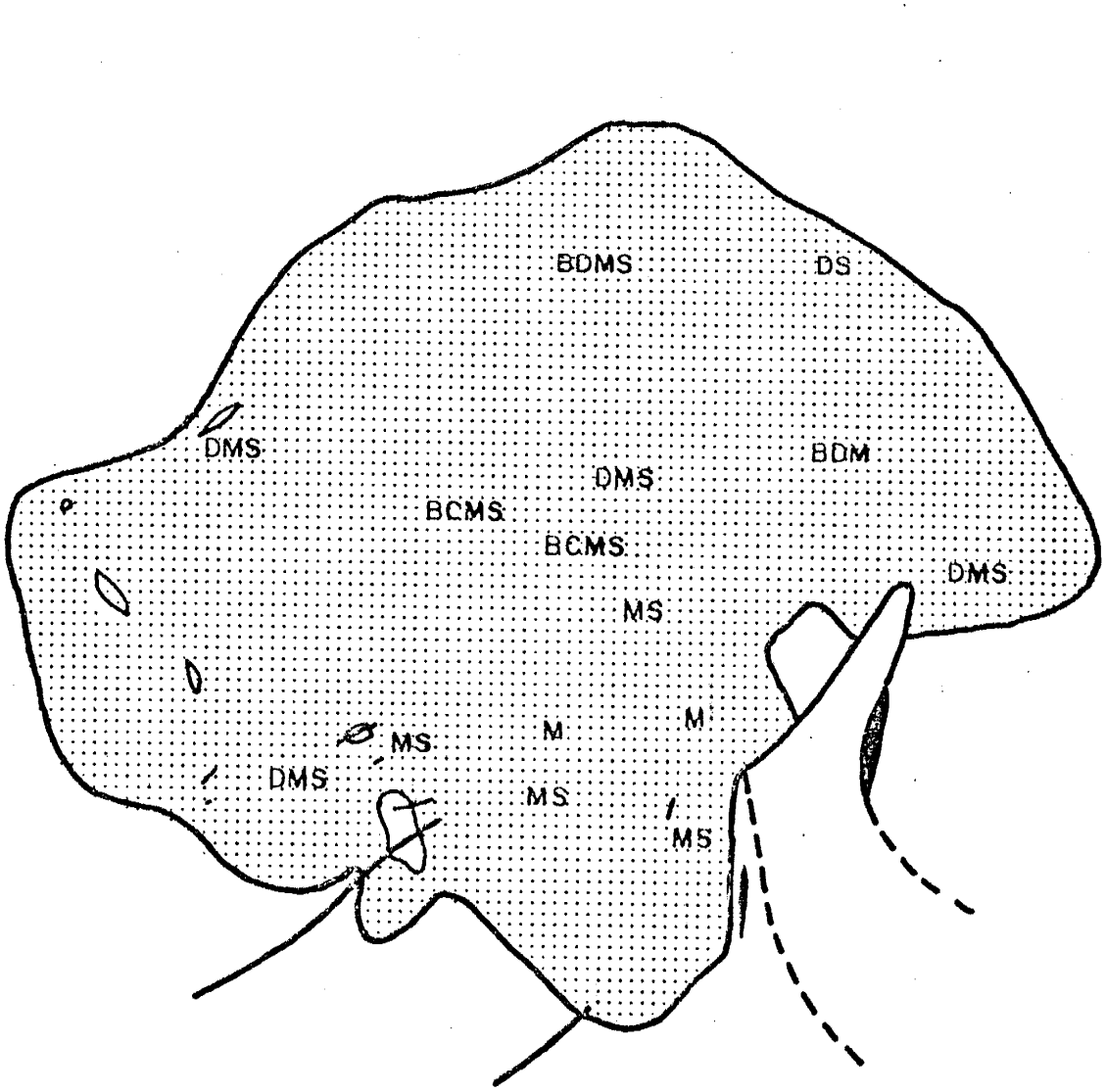
N
BDMS
DS
DMS
BDM
DMS
BCMS
BCMS
DMS
MS
MS
M
M
DMS
MS
MS

Table 1. Major element analysis of the intrusive rocks as weight percent of the oxides.

Sample	S-8	S-10	S-12	S-13	S-19	S- 21
SiO_2	70.1	64.8	64.2	69.2	64.7	64.3
Al_2O_3	13.6	15.5	16.4	13.0	13.6	13.5
FeO	1.3	2.8	4.0	6.9	3.4	3.6
MgO	0.1	0.6	0.6	0.4	1.4	1.1
Na_2O	4.7	5.6	5.0	6.3	5.8	5.5
K_2O	4.2	5.2	5.3	2.7	4.3	4.6
CaO	1.1	1.9	2.5	1.1	2.4	2.7
Total	96.3	96.3	97.9	99.5	95.6	96.2

Sample	S-27	S-29	F-10	3-12	Y-15
SiO_2	68.8	69.8	70.2	63.1	63.0
Al_2O_3	14.0	14.5	13.6	16.9	16.8
FeO	1.6	1.4	1.7	3.6	3.6
MgO	0.1	0.1	0.5	1.3	1.4
Na_2O	4.8	4.6	5.9	4.7	3.9
K_2O	5.1	4.3	4.6	6.0	5.9
CaO	1.3	1.2	1.2	2.6	3.7
Total	96.7	96.9	98.6	98.2	98.3

Table 2. Volume percent normative mineral contents of igneous rock samples from Lone Mountain.

Laccolith	QUARTZ	ORTHOCLASE	ALBITE	ANORTHITE	BIOTITE	DIOPSIDE	MAGNETITE	PLAGIOCLASE (Ab content)	% K-FELDSPAR of total feldspar	Classification
S-8	26.2	26.5	41.6	4.3	-	0.6	0.7	91	37	QM
S-10	10.9	31.8	48.7	3.9	-	3.2	1.6	93	38	QM
S-12	14.4	27.6	41.4	10.9	4.1	-	1.7	80	34	QM
S-13	24.7	14.6	53.9	0.2	-	2.6	3.9	99	21	GD
S-21	14.3	27.0	47.5	2.9	-	6.1	2.1	94	35	QM
S-27	21.2	31.1	41.6	4.1	-	1.0	0.9	91	40	QM
S-29	24.3	27.8	41.2	5.6	-	0.3	0.8	88	37	QM
F-10	19.5	26.6	49.7	0.3	-	3.0	0.9	99	35	QM
Dikes										
3-12	12.0	35.3	39.1	11.5	-	-	2.0	77	39	QM
Y-15	16.2	33.9	31.2	16.6	-	-	2.1	65	41	QM

among the minerals identified in thin section (Appendix A, Table 2). On the basis of the normative mineral compositions the rocks fall along the granodiorite-quartz monzonite composition boundry of Travis (1959), with all but one of the samples falling within the quartz monozonite field. Normative plagioclase compositions, as given in Table 2, average 92 percent albite.

Butler (1964) reported modal orthoclase contents of greater than 90 percent. The normative K-feldspar found in this study, however, averaged only 27 percent. In an attempt to account for this discrepancy between values the thin sections were placed in a potassium feldspar stain (sodium cobaltinitrate) to make the K-feldspar visually distinct. In addition, X-ray diffraction patterns were used to semi-quantitatively compare the peak heights of the various feldspars.

The X-ray patterns show a very strong albite peak at $2\theta = 27.8^{\circ}$ along with a much weaker microcline peak (I = 15-30% of albite peak) at $2\theta = 27.4^{\circ}$. Visual estimates of K-feldspar in the stained slides are in closer agreement with the normative K-feldspar value than with Butler's reported value. Also, the staining revealed that the phenocrysts were not microperthite, as reported by Butler, but rather antiperthite; thin laminae of K-feldspar in an albite host. Because in most samples the phenocrysts comprise 50-80 percent of the rock it is easy to understand how the misidentification of the antiperthite could cause the large difference in K-feldspar percentages.

Dikes.

Dikes found in the immediate vicinity of Lone Mountain are very similar compositionally and texturally to the laccolith and all those sampled have a trachytic porpyritic texture. Where the dikes cut

through the sedimentary rocks, (Fig. 5), they have 1-2 inch chill margins which are not found when the dike cuts the laccolith, indicating the laccolith may have still been relatively hot when the dikes were intruded. Unlike the intrusion of the laccolith, the intrusion of the dikes did not distort the sedimentary rocks through which they cut. Dikes cutting the laccolith are paralleled by sets of closely spaced fractures with the intensity of the fracturing decreasing rapidly within several feet of the dike. Whether the dikes followed the fractures or if the dikes fractured the rocks during their intrusion could not be determined.

Phenocrysts within the dikes are euhedral plagioclase, orthoclase, and quartz. Flagioclase phenocrysts do not contain the small amounts of K-feldspar as did the antiperthite from the laccolith. Sericitization of the plagioclase is very intense, some of the smaller phenocrysts having been totally replaced by fine grained muscovite. Also, there are phenocrysts of deeply embayed quartz which occasionally display overgrowths of microcrystalline quartz, possibly variety chalcedony. The groundmass is composed of lath-shaped feldspar microlites which have an approximate parallel arrangement. In each of the dikes the mafic minerals have been completely altered to limonite, hematite, and carbonates, making it impossible to determine their original mineralogy. Magnetite is found in some samples as minute euhedral crystals dispersed throughout the matrix. Whether this magnetite is primary or hydrothermal could not be determined.

Once again, modal analysis of the samples of dike rock was impractical because of the fine grained matrix, so two samples showing a minor amount of hydrothermal alteration were analyzed chemically for normative mineral calculations. In comparison to the normative mineral

Figure 5. Quartz monzonite dike cutting a limestone bed of the San Andres formation. Tm = tertiary quartz monzonite dike, LMS = limestone bed of the middle San Andres Formation

content of the laccolith the dikes show a slightly higher K-feldspar content and plagioclase with a larger anorthite component (Table 2).

Though the samples often contained iron oxides and oxyhydroxides the only iron bearing mineral used in the distribution program was magnetite because it is the most commonly found iron mineral. Relative amounts of the different iron minerals could not be calculated without having determined ferric and ferrous iron and hydroxide contents. The error resulting from the molar volume differences between magnetite and the other iron bearing phases is minimal owing to their small contribution to the total volume of the rock.

SEDIMENTARY ROCKS

Late Paleozoic and Mesozoic sedimentary rocks exposed in this region are complexly folded in the immediate vicinity of the intrusives. Near the contact of the Lone Mountain laccolith, the sedimentary strata are tightly folded and dip steeply away from the pluton. Yet within a few hundred feet of the contact the beds show no signs of folding and markedly shallower dips than near the intrusive. Three sedimentary rock units are exposed in the study area: San Andres Formation, Bernal Formation, and a Tertiary agglomerate of uncertain correlation, (Plate 1).

San Andres Formation

The Permian San Andres Formation is a sequence of limestone, dolomite, sandstone, and gypsum, the character of which changes drastically over short distances, (F. Kottlowski, personal communication, 1975). The top of the San Andres is an erosional surface which has developed relief on the order of several hundred feet prior to the deposition of the Bernal Formation. In the northern Caballo Mountains (100 miles to the southwest) the San Andres Formation is 780 feet thick and contains about 32% yellowish to pale red sandstones (Kelley and Silver, 1952). Thirty miles to the west, in the Oscura Mountains-Chupadera Mesa area, the formation is dominated by thick gypsum beds (Wilpolt and Wanek, 1951). In the San Andres Mountains (50 miles SSE) Kottlowski, et al. (1956), report a single one foot thick gypsum bed. On the west slope of Lone Mountain Smith (1964) measured 700 feet of an incomplete section of San Andres which was found to contain significant amounts of all the previously mentioned rock types.

The basal section of the San Andres Formation south of Lone Mountain,

as described in detail by Weber (1964), consists of 20-25 feet of gypsum with thin interbeds of grey dolomite and silty, gypsiferous limestone. These beds are overlain by 20-40 feet of friable sandstone and 50 feet of silty dolomite and fossiliferous mottled limestones. The dolomites and limestones are interbedded with gypsum and lenticular quartz sandstones (possibly the Glorieta Sandstone equivalent). The middle San Andres is composed of massive beds of limestone ranging from light to dark grey. Some of the beds are fossiliferous, containing fragments of crinoid stems, gastropods, and coiled cephalopods. Much of the limestone is fetid and contains hydrocarbons. The upper San Andres contains grey limestones interbedded with thin gypsum stringers.

Aerial photographs reveal the frequent formation of sink holes in the San Andres Formation. Near the top of the San Andres, sink holes filled with layers of material from the overlying Bernal Formation indicate the development of Karst topography as early as the upper Permain or Triassic.

Bernal Formation

The Triassic Bernal Formation consists of fine grained clastic material with minor limestone interbeds. The thickness of the formation in the area of Lone Mountain ranges from 200-300 feet. Griswold (1959) correlated these rocks with the Permian Chalk Buff Formation, which overlies the San Andres near Artesia. Smith (1964), however, feels the lithology is more closely related to the overlying Triassic formations rather than the underlying San Andres and therefore places it within the Triassic.

Outcrops of the Bernal are rare as it has a low resistance to erosion and weathering. The Bernal breaks down into bright red soils

which contrast greatly with the dull grey soils formed over the gypsiferous San Andres.

Tertiary Agglomerate

In the southeast corner of the study area there is a limited exposure of a sequence of volcanic sediments. Within the area of investigation the rock is primarily tuffaceous with widely dispersed lenses of sandstone and siltstone. The tuff is a brilliant white and contains abundant kaolinized feldspar phenocrysts. Small pebbles and cobbles of igneous rock resembling that from the Lone Mountain laccolith are scattered throughout.

Smith (1964) describes this sequence in detail from more extensive exposures to the south. The composition of the basal unit varies from a flow breccia with boulder size inclusions of Mancos Shale to a highly indurated sandstone which resembles a quartzite on broken surface. Overlying the basal bed is 375 feet of volcanic agglomerate with interbedded mudstone and sandstone. The total thickness of the unit is estimated to be over 400 feet.

As a result of the isolated occurrence of the agglomerate, correlation to established formations in the surrounding region is very difficult. It is most probable that the agglomerate is a northern extension of the Sierra Blanca volcanic complex. The westerly dipping agglomerate is post Lone Mountain laccolith as it lies in an angular unconformity over the Permian and Triassic formations which are dipping southeast as a result of the intrusion. The agglomerate, however, is cut by a number of small lamprophyre and quartz monzontie dikes, therefore the agglomerate predates the final stages of igneous activity. A tentative age of late Tertiary

has been assigned to this sequence by Smith (1964).

METAMORPHIC ROCKS

The only exposures of contact metamorphic zones are within the various mines and prospects. A thick soil cover precluded determination as to whether or not there was any continuity of the skarns from one location to another around the laccolith. The common occurrence of blocks of diopside and iron ore in arroyos which do not pass near any of the known deposits would suggest that a great deal of skarn remains buried. The following sections will briefly detail the geology, mineralogy, and paragenesis of the skarns exposed in the various mines and prospects at Lone Mountain and shown in Figure 6.

Ferro Mine

On the western slope of Lone Mountain a mineralized roof pendant lying within the quartz monzonite laccolith has been exposed in the workings of the Ferro Mine (Fig. 7). The pendant, approximately 1100 feet long in a NE-SW direction and 10-70 feet wide, contains near vertical beds of gypsum, dolomitic limestone, and quartzite. These beds strike approximately N 35° E, paralleling the general trend of the pendant. A 3-6 foot thick magnetite vein, conformable to the bedding, runs the entire length of the pendant. A zone of diopside mineralization parallels the western side of the magnetite vein (Fig. 8). As shown in Figure 9 the diopside mineralization occurs in both quartzite and quartz monzonite. The eastern edge of the magnetite vein forms a sharp contact with the bed of dolomitic limestone; in several places, however, the contact is broken by a thin zone, 1-2" thick, of selenite crystals. The only evidence of alteration within the limestone are small stringers of recrystal-

Figure 6. Location of mines and prospects in relation to the Lone Mountain laccolith, (stippled area).

A) Yellow Jacket Mine
B) Nameless
C) Nameless
D) Stoddard Mine
E) Nameless
F) Nameless
G) House Prospect
H) Hudspeth Prospects
I) Nameless

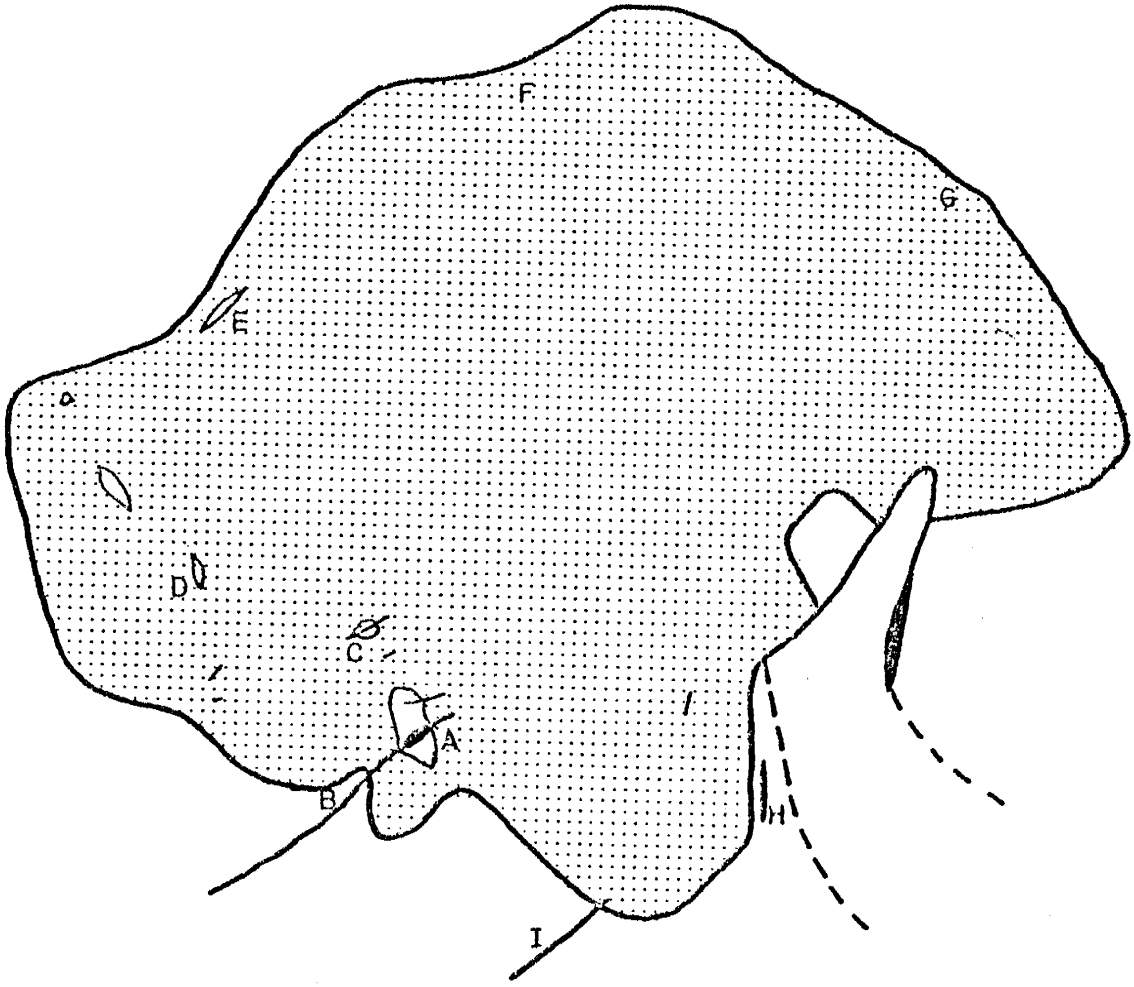
F
G
E
D
C
A
B
H
I

Figure 7. The workings of the Ferro Mine, facing NE., paralleling the trend of the roof pendant.

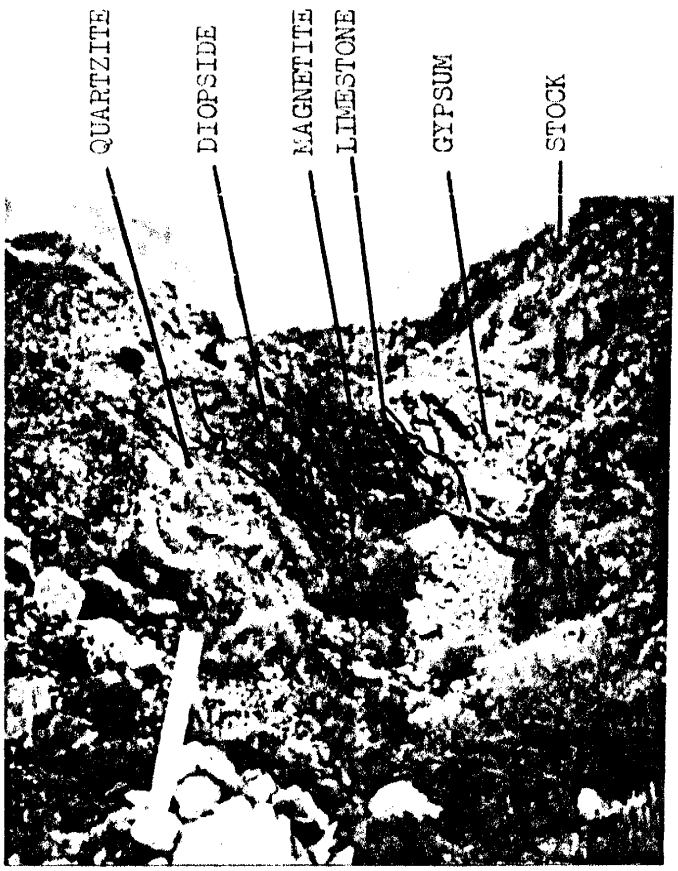

Figure 8. Working face of the Ferro Mine, viewed NE, parallel to the strike of the bedding, showing the relative positions of the sedimentary, igneous, and skarn rocks. The bush in front of the magnetite vein is approximately 2,5' wide.

Figure 9. Schematic plan view of the Ferro Mine roof pendant.

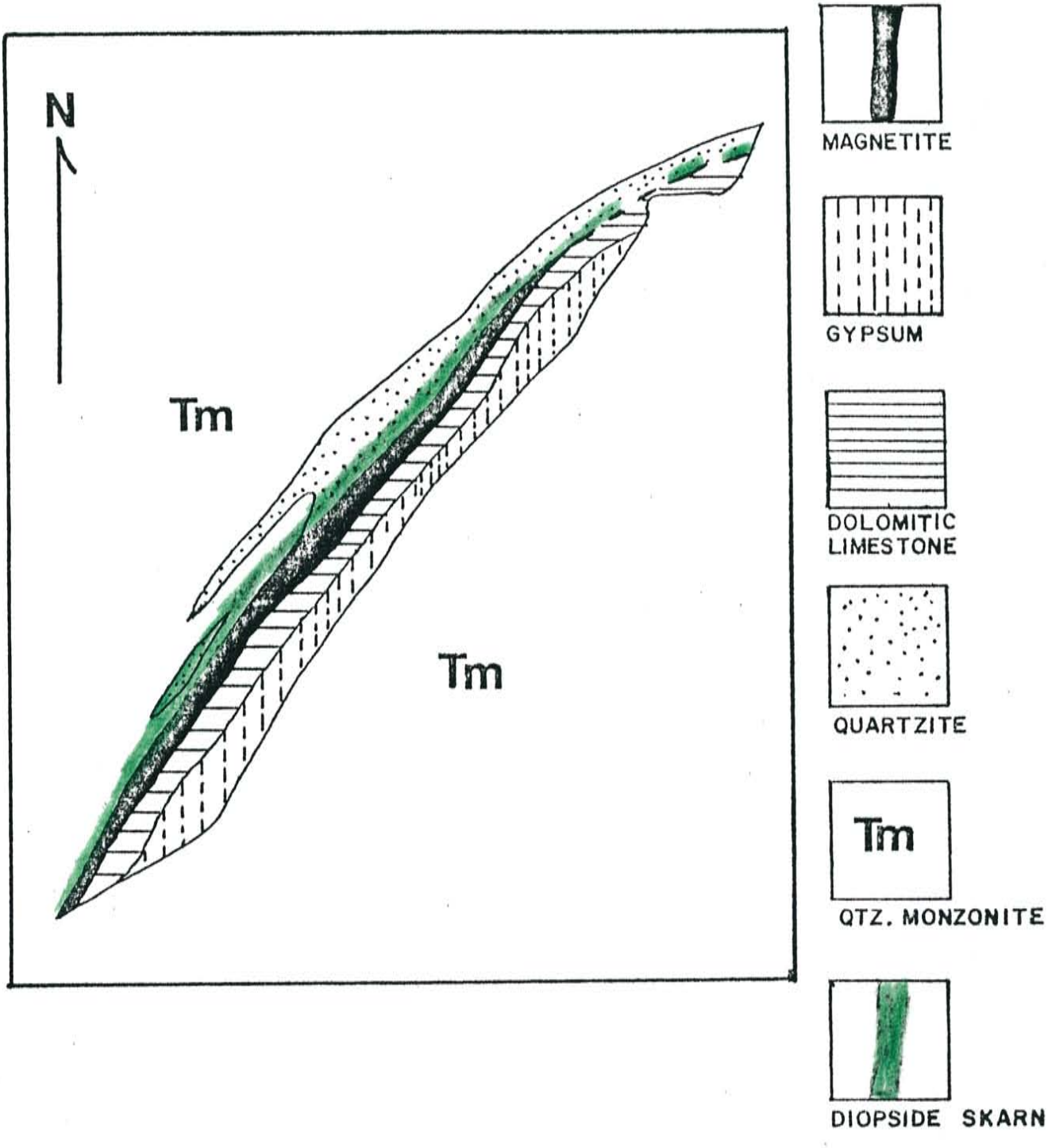
N
Tm
Tm
MAGNETITE
GYPSUM
DOLOMITIC LIMESTONE
QUARTZITE
Tm
QTZ. MONZONITE
DIOPSIDE SKARN

lized calcite. Neither diopside nor any other silicate is found in the dolomitic limestone.

The skarn can be divided into three zones on the basis of mineralogy; diopside, diopside + nontronite, and magnetite. The mineralogy of the diopside zone is predominately diopside with smaller amounts of phlogopite, calcite, tremolite, and magnetite. Calcite is found as small 1-2 inch irregular masses intergrown with the diopside. Small flakes of phlogopite are found throughout this zone but probably constitutes less than one percent of the rock. Small veins of fine accicular tremolite randomly cut through the zone. Anhedral magnetite was observed in thin sections as interstitial growths between crystals of diopside.

A 1-3 inch layer of limey-green, fine grained, friable rock lies between the diopside and magnetite zones. Minerals identified by X-ray diffraction methods were nontronite, diopside, plagioclase, phlogopite, and magnetite. Red streaks of hematite were observed in the porcelain mortar in which the sample was crushed, yet a hematite pattern was not detected by X-ray diffraction.

The iron ore is predominately magnetite with small crystals of specularite dispersed throughout. Pyrite was found in samples collected from a rock pile adjacent to the working face of the mine but was not observed in outcrop. Under magnification the pyrite appears rounded with investments of magnetite. Also the pyrite is commonly associated with patches of geothite.

The approximate paragenetic sequence for the Ferro Mine is given in Table 3. The paragenetic relationships of the minerals in the diopside + nontronite zone could not be determined because their

Table 3. Approximate paragenetic sequence for three skarns at Lone Mountain.

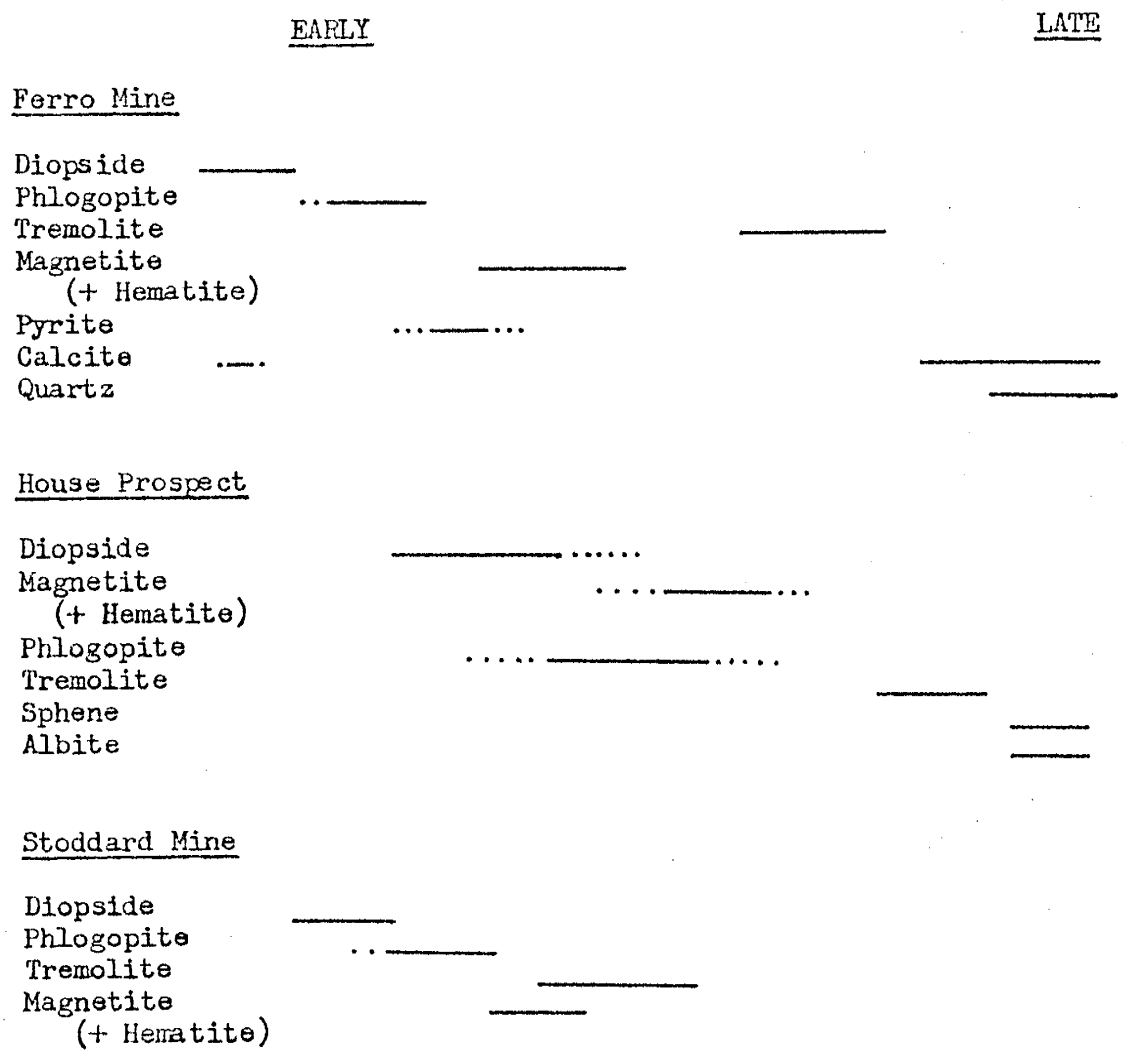

very small size prevented accurate visual observation.

House Prospect

The House Prospect is a small magnetite deposit located on the northeast slope of Lone Mountain. Exposures are very poor in the area owing to dense underbrush and a thick mantle of soil. The deposit, which lies within the soil zone, consists of scattered boulders of magnetite and gypsum within a clayey soil. An adit driven into the hillside above the prospect penetrates about 15 feet of soil before reaching the quartz monzonite laccolith.

At the border between the soil and the igneous rock is a 3-4 foot zone of diopside with small pods of magnetite. This grades quickly into quartz monzonite with numerous closely spaced veinlets of diopside. According to Butler (1964) the diopside veinlets are found along the entire 50 foot length of the adit. A small pit 75 feet east of the adit contains numerous blocks of a brecciated quartz monzonite with a diopside matrix, (Fig. 10). A fresh exposure of this breccia was not found.

Field and petrographic evidence indicates that the diopside forms an endoskarn within the quartz monzonite. No exposures of an exoskarn could be found, possibly owing to the advanced weathering of the area. However, the pods of magnetite in the diopside could not be the source of the large 4-5 foot boulders of magnetite found in the soil.

The mineralogy of the endoskarn, which has replaced the quartz monzonite is rather simple. The rock is composed almost entirely of dark green diopside with smaller amounts of phlogopite, tremolite, sphene, and albite. Chemical analysis of a diopside crystal and a sample of the skarn are listed in Table 4. The diopside composition

Figure 10. Breccia found in a pit near the House Prospect with blocks of quartz monzonite from the laccolith in a diopside matrix.

Table 4. Chemical analysis of individual diopside crystals and whole rock samples of diopside skarn; listed as weight percent of the oxides.

Crystals:

	SiO_2	Al_2O_3	FeO	MgO	Na_2O	K_2O	CaO	MnO
House	54.4	-	5.8	11.4	0.5	0.1	26.9	0.9
Stoddard	54.9	-	8.5	10.2	0.4	0.6	24.3	0.6
Mine C	52.2	-	2.7	16.2	0.8	0.1	26.7	1.2

Whole rock:

	SiO_2	Al_2O_3	FeO	MgO	Na_2O	K_2O	CaO	MnO
House	54.6	-	6.4	12.2	1.2	0.3	23.2	0.9
Yellow Jacket (north)	55.4	-	5.1	13.2	0.5	0.1	23.0	0.7
Yellow Jacket (central)	54.2	-	9.0	9.8	1.6	0.2	22.8	0.9

in terms of the solid solution end members is 75% diopside, 21% hedenbergite, and 4% johannsenite.

Tremolite is found as an asbestiform coating on diopside crystals. One to two millimeter crystals of sphene and 5-10 mm crystals of albite have also grown on the surface of the diopside. The magnetite contains crystals of phlogopite and diopside but no tremolite or sphene. X-ray diffraction of the ore samples indicate the presence of both magnetite and hematite. By the cursory examination of slabbed samples under low magnification the hematite is seen throughout the ore as aggregates of specularite crystals within the magnetite. The approximate paragenetic sequence for the House Prospect is given in Table 3.

Walker and Osterwald (1956) reported finding the uranium mineral metatorbenite in the ore. Examination of the ore samples failed to support these findings. Butler (1964) did not detect any uranium during his chemical analysis of the ores.

Yellow Jacket Mine

The largest roof pendant within the laccolith is exposed in the workings of the Yellow Jacket Mine one the south slope of Lone Mountain. The pendant is composed of contorted beds of fetid limestone and gypsum. Boulders of quartzite are found on the surrounding hillsides but not in the mine area. The beds at the eastern laccolith contact are oriented N 9° E; 60° NW, yet are nearly flat lying within a few feet of the contact (Fig. 11). The geology of the pendant is complicated by the presence of numerous dikes and sills of quartz monzonite ranging from ten's of feet to only a few inches thick which cut the sedimentary rocks and the laccolith.

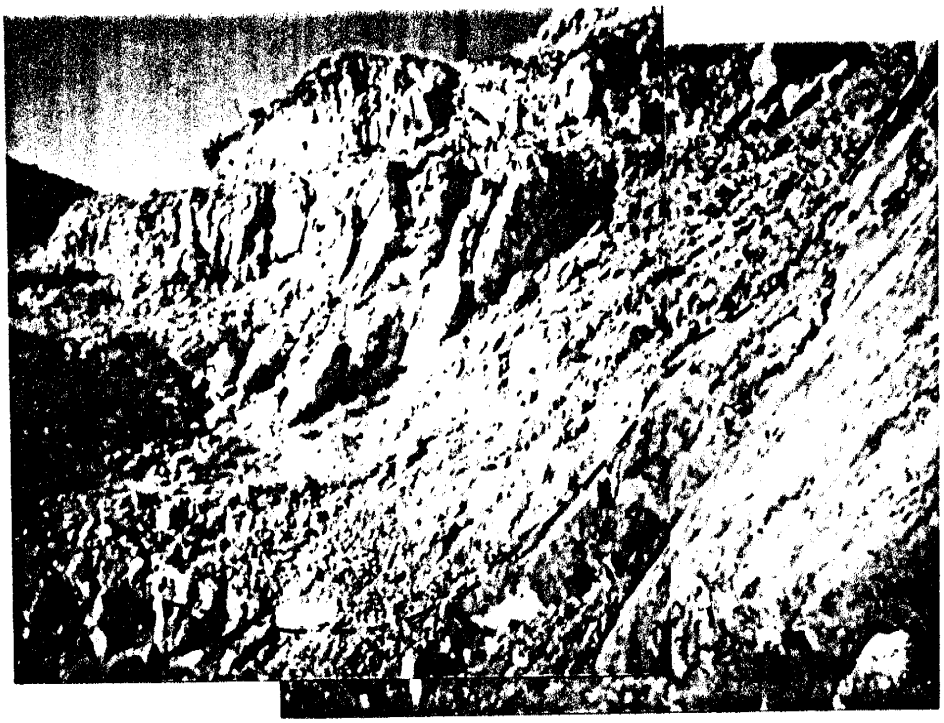

Figure 11. Steeply dipping, dark grey fetid limestone unit lying conformable to the igneous contact and flat lying at the bottom of the picture. Dashed line follows approximate top of the limestone bed.

The Yellow Jacket is actually a group of three mines which lie along an approximate N-S line within the pendant. The central deposit which is predominately hematite ore is the largest. On either side of this mine lie smaller magnetite deposits (Fig. 12). The key areas between the excavations are obscured by soil and dumps, making it impossible to determine the lateral variations within the pendant. The remaining discussion of the Yellow Jacket will be divided into a brief description of each of these mines.

The northern end of the pendant is cut by a 15 foot thick, E-W trending dike. A deep trench normal to the north side of the dike, cuts through 25 feet of diopside skarn and 15-20 feet of magnetite ore before reaching the dike. The magnetite ore is very dense with scarce patches of silicates and hematite. The diopside skarn contains small amounts of phlogopite, magnetite, and tremolite. On the opposite side of the dike, a trench driven from the south cuts through a near vertical bed of unaltered limestone and a 3-4 foot thick vein of magnetite. The results of a chemical analysis of the diopside skarn is given in Table 4.

The sedimentary beds are highly contorted into a series of tight drag folds within the southern end of the pendant. A single pod of magnetite 2-3 feet in diameter and of unknown length is exposed in the wall of the excavation. Approximately 10 feet north of the magnetite pod a zone of diopside is partially exposed. No outcrops of dikes or sills were found in the mine. The complex folding and limited exposures prevented the determination of the relationship of the two zones to the sedimentary and igneous rocks.

The centrally located hematite ore body was mined by the open

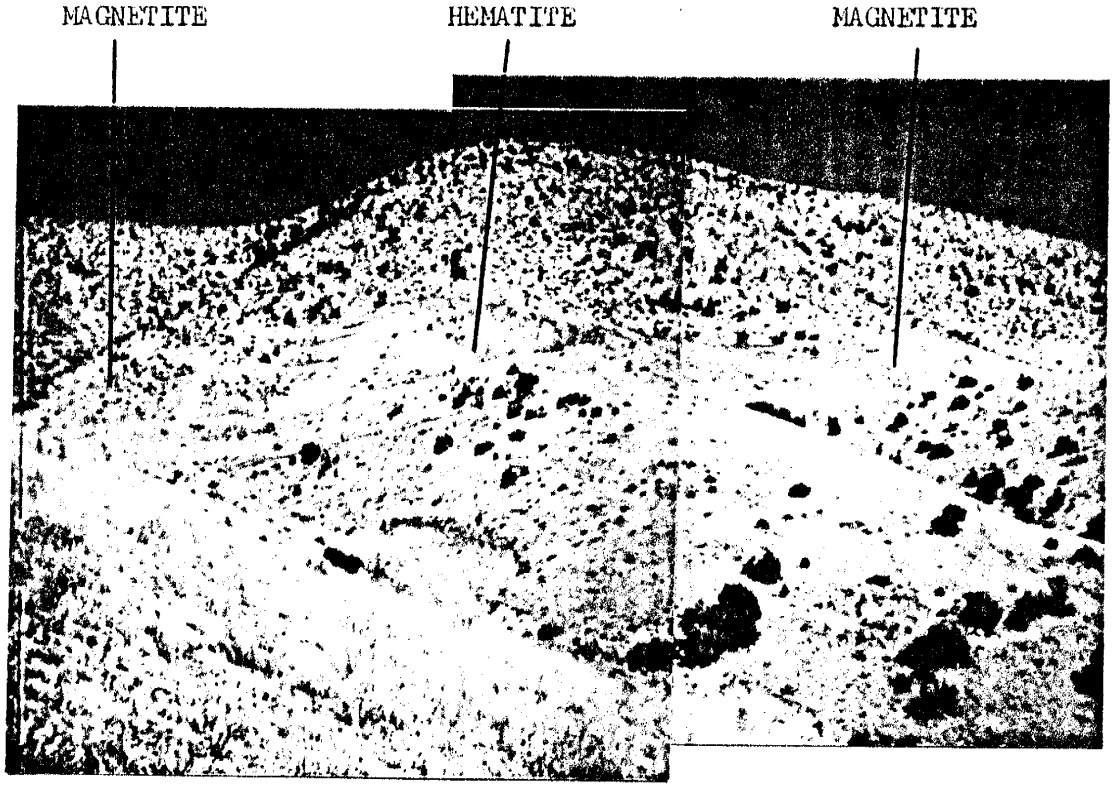

Figure 12. Yellow Jacket Mine, facing northeast, showing the relative positions of the magnetite and hematite deposits.

pit method; the bottom of the pit penetrating the top of a sill. A NE-SW trending 10-15 foot thick vertical dike is exposed in the benches along the northern wall of the pit; Figure 11 shows the attitude of the beds in relation to the igneous contacts. A dark bed of fetid limestone lies conformable to the high angle contact and then quickly levels out near the bottom of the mine. The highest concentration of ore lies along the contact of the sill with the limestone. A small lens of ore lies along the contact between the laccolith and the limestone but its thickness decreases quickly and eventually pinches out with increasing distance from the sill.

Within the upper 4-6 inches of the laccolith an endoskarn of silicate minerals has replaced the quartz monzonite; limestone at the contact has been recrystallized and is cut by veins of limonite, hematite, and siderite. The endoskarn changes with increasing depth from diopside to silicified quartz monzonite to relatively fresh quartz monzonite. Thin sections of the apparently unaltered rock revealed, however, that the groundmass is being destroyed by silicification and that the quartz phenocrysts are replaced or enveloped by diopside (Fig. 13). A chemical analysis of a sample of the diopside skarn is given in Table 4.

Where the previously mentioned lens of hematite lies adjacent to the laccolith, the zoning in the endoskarn becomes nontronite + talc + quartz, to pure diopside, to silicified quartz monzonite, to relatively unaltered rock with increasing depth into the laccolith.

No evidence could be found which would suggest that these minerals did not form simultaneously, with the exception of calcite which is

Figure 13. Quartz phenocryst in the quartz monzonite laccolith enveloped by diopside, planar light, X100. Q = quartz, D = diopside

found lining cavities within the hematite ore. However, because the ore lies adjacent to the dikes and sills and because the relative intensity of the diopside mineralization is greatest near the same, the mineralization appears to have coincided with the intrusion of the dikes and sills rather than the laccolith.

Stoddard Mine

Another roof pendant within the laccolith has been exposed in the Stoddard Mine on the southwest slope of Lone Mountain. The sedimentary beds were complexly folded and fractured during the intrusion of the laccolith. One quartzite unit exposed within the southeast end of the mine, (point X in Fig. 14) was oriented S 33° E; 55° SW. This same unit can be traced to a point approximately 50 feet northwest (Y in Fig. 14) where it is oriented 90° to the previous location and dips 15° NW.

Figure 15 is a composite stratigraphic section for the sedimentary units exposed in the Stoddard Mine. The uppermost vein of magnetite can be traced laterally to a bed of dolomitic limestone, indicating that this vein and probably the one below it, have replaced limestone beds.

A collapse breccia (characteristic of the San Andres Formation in this region) is exposed in the walls of the northeast end of the mine. The breccia zone is approximately 20 feet wide and contains large randomly oriented boulders of gypsum and limestone. The thin beds of quartzite probably represent small lenses of sandstone such as are found in the lower San Andres.

Mineral zoning is not as obvious as in the other mines around the laccolith as a result of the greater variations in lithologies

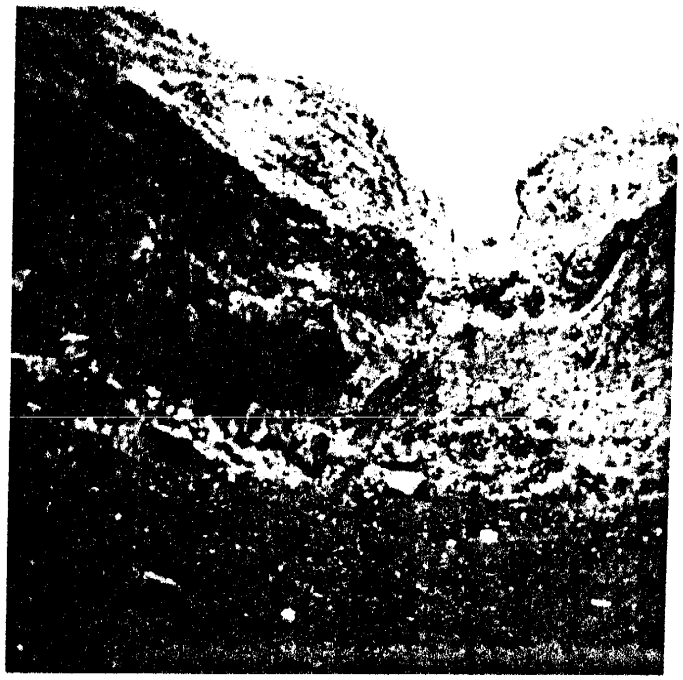

Figure 14. The Stoddard Mine as viewed from the southeastern end of the mine. A quartzite unit at X is oriented at 90° to the same unit at Y.

Figure 15. Composite stratigraphic section for the Stoddard Mine.

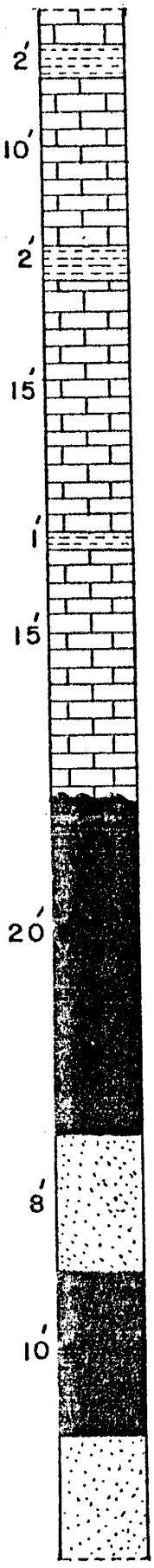

- limestone
2′ - shale
10′ - limestone
2′ - shale
15′ - limestone
1′ - shale, chlorite-montmorillonite mixed layer
15′ - dolomitic limestone
20′ - magnetite with minor silicates
8′ - quartzite
10′ - magnetite with minor silicates
- quartzite, grades laterally into tremolite rock

and the intense folding. The minerals which have been verified in the Stoddard Mine are diopside, tremolite, phlogopite, magnetite, and hematite.

As previously noted one of the two magnetite veins can be traced laterally to a dolomitic limestone. Both the ore and the limestone contain small pods of phlogopite and diopside. The silicates apparently formed first, with the surrounding rock later being replaced by magnetite.

The lower quartzite bed has been mineralized to varying degrees. Thin sections reveal the following changes in mineralogy in samples taken progressively closer to the overlying magnetite vein, (Figs. 16, 17, and 18).

QUARTZ → QUARTZ + DIOPSIDE → TREMOLITE

The approximate paragenetic sequence for the Stoddard Mine is given in Table 3.

Hudspeth Prospects

The Hudspeth Prospects consist of a pair of bulldozer cuts within the southwestern slope of Lone Mountain. Unlike the deposits discussed so far, these do not lie within roof pendants. Mineralization, in the form of magnetite and small amounts of diopside, lies adjacent to a small quartz monzonite dike within the San Andres limestone, 20 feet from and parallel to the laccolith-sedimentary contact.

Miscellaneous Mines and Prospects

The following section is devoted to the smaller prospects and mines which have not been noted in any published reports. The mines will be referred to by the letter signifying their location in Figure 6.

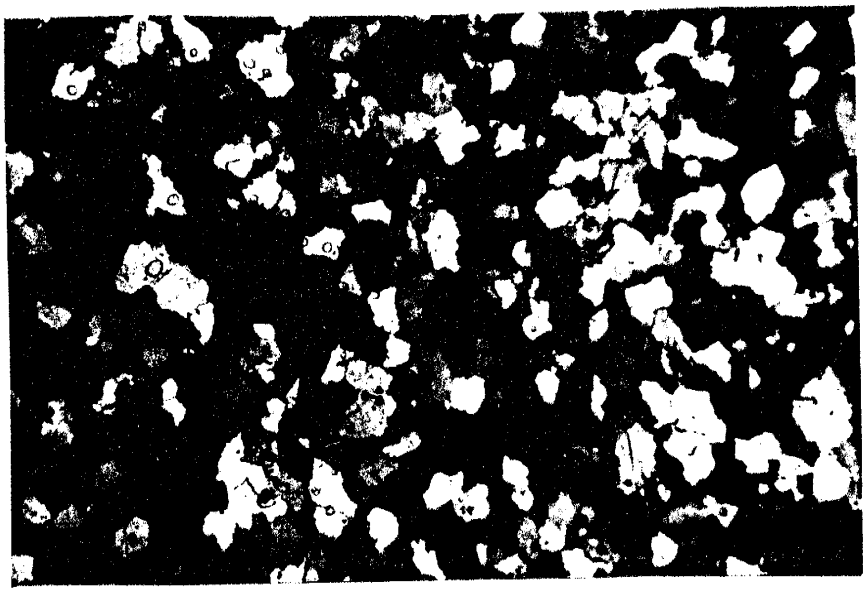

Figure 16. Unaltered quartzite from the Stoddard Mine, X-nicols, X25.

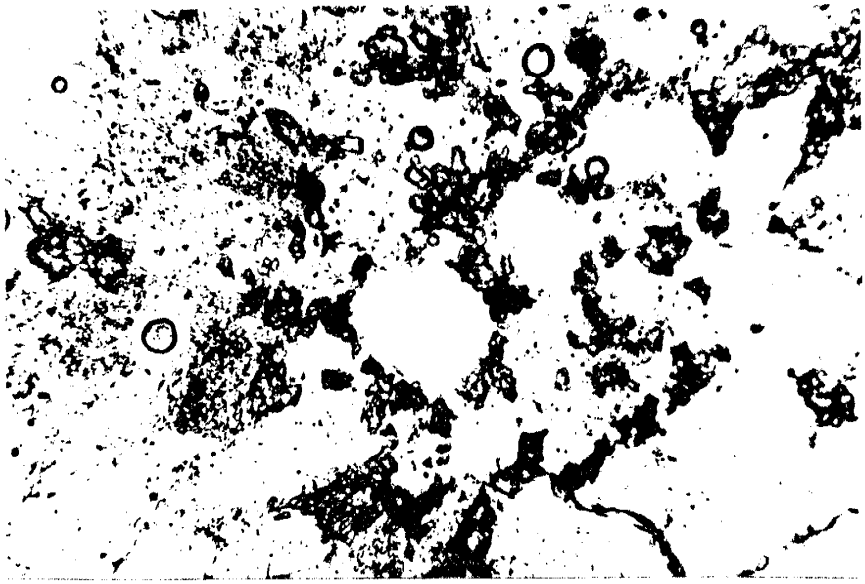

Figure 17. Quartzite with interstitial diopside (grey, high relief), planar light, X100.

Figure 18. Pure tremolite rock which has replaced a quartzite in the Stoddard Mine, X-nicols, X100.

Mines B and I are the only workings found outside the influence of the laccolith. The ore, consisting of massive hematite; specularite; and minor amounts of magnetite, lies adjacent to quartz monzonite dikes in limestone beds of the San Andres Formation. No silicate minerals were found in either mine. Fracture surfaces within the ore are occasionally coated with thin films and rare crystals of a copper sulfate mineral, brochantite(?). A thin layer of limonite lies between the hematite ore and the limestone, indicating the oxidation of pyrite. Thin stringers of white recrystallized calcite within the grey, fine grained limestones occasionally parallel the contact.

Mine C is a small magnetite deposit within a roof pendant of tightly folded limestone and gypsum. A 12 foot thick quartz monzonite dike trending ENE cuts through the pendant, and the magnetite lies adjacent to it bounded by a zone of diopside. Immediately north of the pendant, a series of approximately N-S trending veins of diopside and magnetite lie within the laccolith. The diopside forms very large crystals, 1-2 inches long. A chemical analysis of one of the crystals is given in Table 4. In terms of the compositional end members the crystal contained 88% diopside, 8% hedenbergite, and 4% johannsenite. Specularite is found frequently on fracture surfaces within the surrounding laccolith.

The mineralization within mine F is quite similar to that found in the other magnetite deposits. However, in this case the mineralization has taken place entirely within the quartz monzonite laccolith. No evidence of a roof pendant or dike could be found. The mineralization occurred within a highly fractured zone, suggesting the

presence of a dike at depth. The mineralized zone consists of a 3 foot thick vein of ore bounded on either side by several feet of diopside. The ore is a coarse crystalline magnetite with ½-1 inch long hexagonal crystals of dahllite, a carbonate-hydroxylapatite.

GEOCHEMISTRY

The remainder of this investigation will be devoted to the determination of the probable genesis of the deposits and composition of the mineralizing solutions based upon the geologic and mineralogic relationships reported earlier in this paper.

The skarns at Lone Mountain can be divided into two types based upon the mineralogy of the dominant iron oxide present; magnetite or hematite. Within each of the groups the skarns show a mineralogical uniformity. Because of this uniformity, it seems safe to assume that their origins were also similar. Therefore, the following discussions will be primarily limited to the two largest mines, the Yellow Jacket and Ferro Mines, as they provide the most information through exposures and are felt to be most representative of the hematite and magnetite bearing skarns, respectively.

Three variables control the stability of a mineral interacting with an aqueous solution; temperature, pressure, and the chemical composition of the solution. In order to discuss the geochemical environment during the formation of a hydrothermal ore deposit, values or at least reasonable limits, must be assigned to each of the thermodynamic variables.

In working with extinct hydrothermal systems, direct measurement of the temperature, pressure, and solution composition are no longer possible. Therefore the deposits must be examined closely for any evidence which might give some indication of the nature of the hydrothermal systems from which they formed. At times, the value of the evidence presented may be debated on the grounds of its accuracy. However, until a means of determining more reliable data can be

found, this evidence must be used. To have even a vague idea of the temperature, pressure, or chemistry of a hydrothermal system is much more desirable than having no idea at all.

The following three sections specify the process by which approximate values or limits for temperature, pressure, and aqueous solution composition were obtained for the hydrothermal system which existed at Lone Mountain during the formation of the iron deposits.

Temperature

The temperatures during the formation of the ore deposits were determined almost exclusively by fluid inclusion homogenization temperatures. Samples of milky calcite were obtained from the diopside zone within the Ferro Mine and the hematite zone of the Yellow Jacket Mine. The Ferro calcite occurs as irregular blebs 1-2 inches in diameter within the diopside rock. The blebs contain large flakes of specularite and stuby microscopic crystals of diopside. The combination of the relationship of the calcite to the diopside rock and the diopside and hematite crystals within the calcite suggests that the calcite is cogenetic with the skarn mineralization. The Yellow Jacket calcite formed as ½-3/4 inch linings in vugs within the hematite ore. Once again specularite flakes formed within the calcite but no silicates were observed. The exact time of the appearance of the calcite relative to the skarn mineralization is uncertain. In addition, one sample of quartz, also from the Ferro Mine, was analyzed. The quartz was found as 1-2 inch crystals lining a large vug in the rock. The crystals were coated with siderite and drusy quartz. As with the calcite from vugs within the Yellow Jacket Mine, the paragenetic relationships of the quartz are uncertain.

Two samples from each location were analyzed, and each inclusion was run a second time in order to determine whether any leakage had taken place during the first run. All inclusions contained a gas and a liquid phase; no solid phases were observed. Table 5 is a summary of the fluid inclusion homogenization temperatures. In addition, a fluorite sample from a vug within the central part of the Yellow Jacket Mine gave a temperature of 247°C, (R. Beane, personal communication, 1976).

The temperatures obtained place both skarns within the range of 245° - 260°C during the mineralization. The samples taken from vugs show slightly lower temperatures than the contemporaneous calcite from the Ferro Mine. The difference, however, is negligible. These temperatures are based upon the temperature required for the liquid to expand sufficently to fill the inclusion. However, a true temperature of formation would have to be that temperature at which the pressure created within the inclusion by the expanding liquid would equal the pressure during its formation. In the following section an approximate pressure of formation will be determined. With this information the additional temperature needed for the Lone Mountain fluid inclusions to reach the pressure of formation can be calculated.

It should be noted that the fluid inclusions yielded consistent temperatures within and between samples and that the inclusions had similar fluid to vapor ratios. Had boiling occurred during mineralization, two distinct groups of fluid inclusions would have formed, one with high fluid/vapor ratios and one with low ratios. Therefore, the confining pressure must have been large enough to prevent the

Table 5. Fluid inclusion homogenization temperatures determined for samples from the Yellow Jacket and Ferro Mines.

Ferro Mine		
Host: Calcite (3 sample locations)*	1	262°C, 259
	2	257, 255
	3	245, 251
Host: Quartz (1 sample location)	1	245, 248
Yellow Jacket Mine		
Host: Calcite (2 sample locations)	1	250, 252
	2	249, 246

* Two samples from each sample location were analyzed.

formation of a vapor phase.

Pressure

It is difficult to determine the exact pressure once exerted on a hydrothermal system. Methods are available, however, by which upper and lower limits on pressure can be calculated.

A maximum confining pressure may be determined by estimating the thickness of the overburden during the time of mineralization. The Lone Mountain pluton and dikes were intruded during the early- to mid-Tertiary into the lower units of the San Andres Formation. The youngest stratigraphic unit present at that time was probably the Cub Mountain Formation. The amount of overburden, therefore, consisted of the sum of the thicknesses of all those stratigraphic units lying between the bottom of the San Andres and the top of the Cub Mountain.

Griswold (1959) lists the approximate thicknesses of these units in Lincoln County. The greatest thickness given for a formation is used in order to assure that the maximum possible pressure has been derived (Table 6). The maximum thickness of the overburden derived in this manner is 1.5 kilometers. In terms of pressure the overburden would exert a maximum lithostatic pressure of 390 bars assuming a density of 2.6 gr/cc or a maximum hydrostatic head of 140 bars assuming the density of water is 1. Owing to the extensive fracturing of the sedimentary rocks in the vicinity of Lone Mountain it is most probable that water would move freely through the rocks and therefore the hydrostatic head provided the pressure on the system.

In the previous section it was noted that the mineralizing solutions were under a confining pressure great enough to prevent boiling. Figure 19 is a plot of the equilibrium P-T curve for liquid

Table 6. Maximum limit on pressure as determined by estimating overburden.

		Maximum Thickness*
Tertiary	Cub Mountain Formation	2000 ft.
Cretaceous	Mesaverde Group	500
	Mancos Formation	400
	Dakota Formation	175
Triassic	Dockum Group	500
	Bernal Formation	350
Permian	San Andres Formation	1000
TOTAL ESTIMATED OVERBURDEN	**********	4925 ft.

Hydrostatic Pressure

1 kilometer column of water = 96.8 atm = 98 bars

4925 ft. = 1.5 km. = 140 bars

Lithostatic Pressure

Assume average specific gravity of rocks = 2.6

1 km. of rock = 260 bars

1.5 km. = 390 bars

*Values from Griswold, 1959.

Figure 19. Equilibrium P-T curve for water and steam, (Allmendinger, 1976).

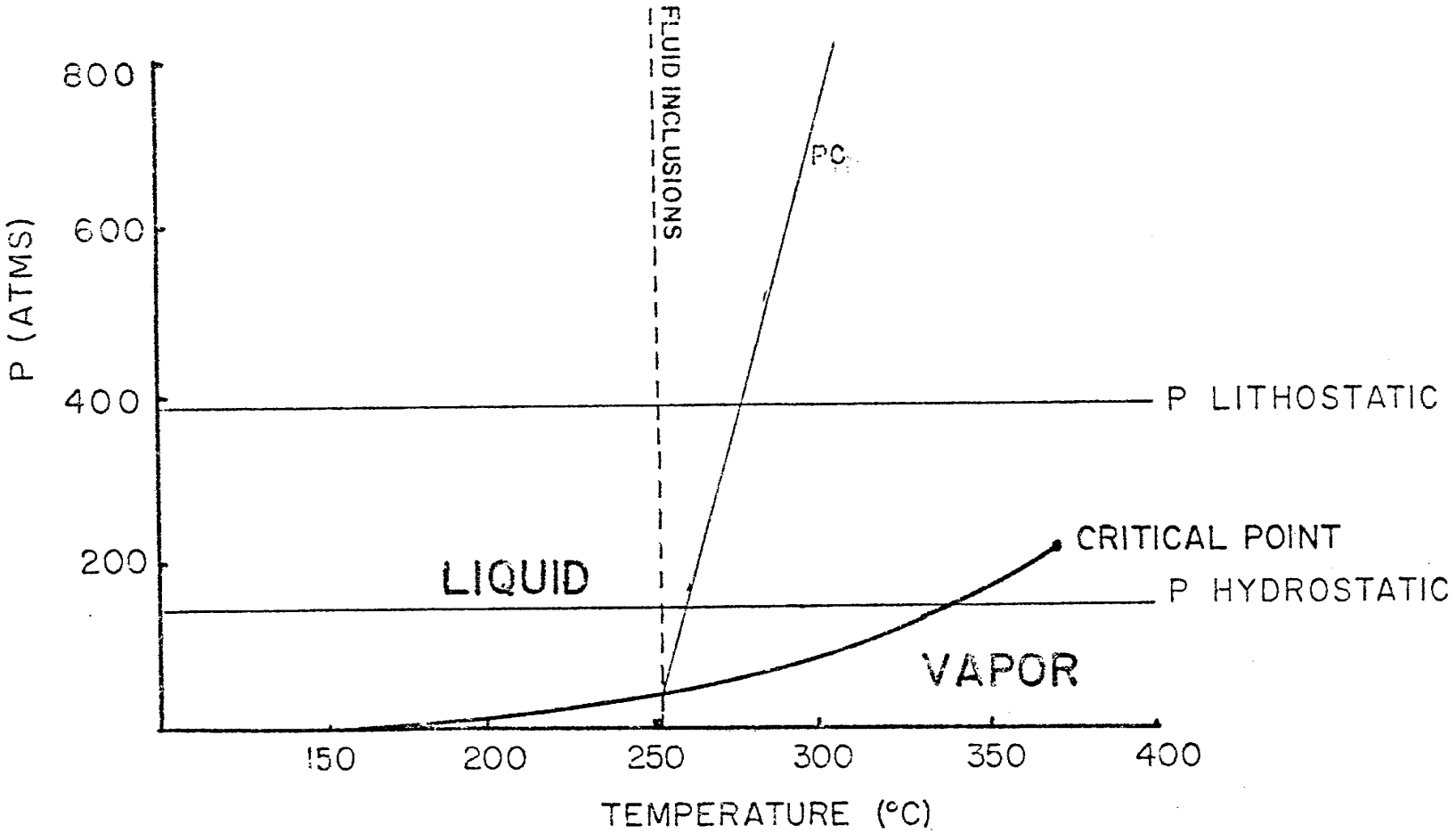
800
600
400
200
P (ATMS)
FLUID INCLUSIONS
PC
P LITHOSTATIC
CRITICAL POINT
LIQUID
P HYDROSTATIC
VAPOR
150
200
250
300
350
400
TEMPERATURE (°C)

water and steam. At the approximate temperature of mineralization, 250°C, the minimum pressure needed to prevent boiling is 45 bars. In turn, with a maximum pressure of 140 bars the maximum temperature without boiling is about 340°C.

Line PC in Figure 19 is the path of constant density for pure water through P-T space. The presence of soluble salts in the liquid will change the slope of the line, but at 140 bars and an initial homogenization temperature of 250°C the line is offset only one degree by a 5 wt. % NaCl solution. Using the approximate Lone Mountain fluid inclusion homogenization temperature of 250°C and a pressure of formation at 140 bars, the true temperature of formation would then be 255°C. Therefore, the actual temperatures of formation of the fluid inclusion samples listed in Table 5 should be approximately 5 degrees higher than the given values.

Solution Composition

When limestones and dolomites, which formed under earth surface conditions, are subjected to the pressures and temperatures associated with igneous intrusions they must undergo various changes which will keep them in equilibrium with the new environment. Commonly, the original minerals within these rocks are destroyed, to be replaced by a new mineral assemblage which is stable under the new conditions. The formation of a new mineral assemblage in order to attain equilibrium at a new temperature and pressure may be accomplished by either isochemically redistributing the components within the rock or by removal and addition of components through the introduction of an external aqueous phase not in equilibrium with the mineralogic environment, (ie. metasomatism). A comparison of the chemical

compositions of host rock versus skarn was made to determine whether the formation of contact metamorphic deposits at Lone Mountain were formed isochemically or by metasomatism.

The thickness of sedimentary units were observed to remain constant as they grade laterally into skarn. Therefore, the mineralization of the unit apparently was not accompanied by a change in volume. Which is to say that 100 cc of the sedimentary rock is equivalent to 100 cc of skarn. This, however, does not suggest that the weights and porosities of equal volumes of the two rocks are the same.

If the mineralization was isochemical the number of moles of a component within 100cc of host rock and skarn must be equal. If, however, the mineralization was by metasomatism the moles of component within equal volumes of skarn and host will change according to whether the component was added or removed by the solution.

Earlier in this paper a mineralized quartzite bed within the Stoddard Mine was shown to have developed the following zonation.

QUARTZ - QUARTZ + DIOPSIDE - TREMOLITE

Whole rock chemical analysis was performed on samples from each of the zones, (Table 7). Bulk densities of the samples, (mass divided by the volume of the sample, including pore space), were determined in order to calculate the mass of a 100cc volume of rock. The following formula is used to calculate the number of moles of an oxide component within 100cc of a sample.

$$\frac{\text{Moles oxide}}{\text{100cc rock}} = \frac{\text{(Mass of 100cc of rock) (\% oxide from analysis)}}{\text{(Molecular wt. of the oxide) x 100}}$$

Figure 20 is a plot of moles of CaO, MgO, and SiO_2 for each of the samples as a function of the relative distances between sample

Table 7. Major element analysis of skarn samples from the Stoddard, (ST), and Yellow Jacket, (Y), mines.

Sample	ST-4A	ST-4B	ST-4C
SiO_2	97.0	92.0	58.4
Al_2C_3	-	-	-
FeO	1.4	1.4	3.2
MgO	0.4	2.0	19.9
Na_2O	0.9	1.3	2.6
K_2O	0.1	0.1	0.6
CaO	-	2.9	12.8
MnO	-	-	-
Total	99.5	99.7	97.5

Sample	Y-21	Y-26
CaO	56.1	56.6
MgO	0.7	0.7
FeO	0.3	0.4
MnO	-	0.1
CO_2	40.5	45.1
Insoluble Residue	0.1	0.1
Total	97.7	103.0

Figure 20. Mass transfer within a quartzite bed in the Stoddard Mine. Total distance between ST-4A and ST-4C is 8 feet. The relationship of the samples to the igneous contact could not be determined.
ST-4A = quartzite, ST-4B = quartzite with interstitial diopside, ST-4C = tremolite.

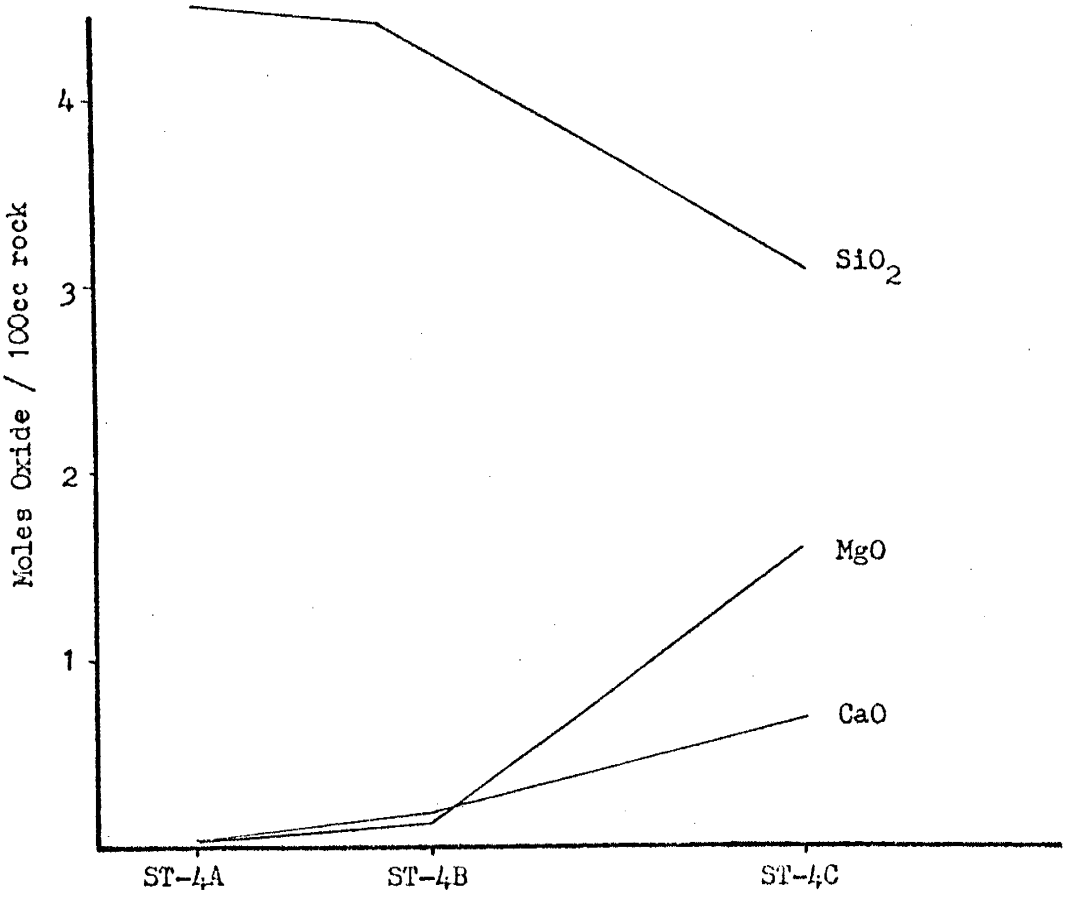
Moles Oxide / 100cc rock
4
3
2
1
SiO2
MgO
CaO
ST-4A
ST-4B
ST-4C

locations, normal to the zone boundries. With the increasing mineralization the quartzite shows increasing amounts of CaO and MgO, with a steadily decreasing amount of SiO_2. Figure 21 is a plot of the same oxides for samples collected across the skarn within the Yellow Jacket Mine. Once again the skarn shows a decrease in SiO_2 accompanied by increasing CaO and MgO relative to the original rock composition.

From these samples it should be apparent that the mineralization must have resulted from the action of hydrothermal solutions in disequilibrium with the original host rocks. Isochemical metamorphism could not account for the drastic differences in the moles of components between host rocks and skarns.

Having determined that the mineralization was initiated by an aqueous phase at 250°C and low pressure, we can examine the stability of the skarn minerals in terms of the composition of the coexisting aqueous phase.

The calcium-magnesium-silicates, diopside and tremolite, are the dominant silicate skarn minerals in all the deposits. The stabilities of these minerals are dependent upon the activities of Ca^{++}, Mg^{++}, H^{+}, and H_4SiO_4 as shown by the dissolution of diopside,

$$CaMgSi_2O_6 + 4H^{+} = Ca^{++} + Mg^{++} + 2H_4SiO_4$$

for which

$$K_s = \frac{(Ca^{++})}{(H^{+})^2} \frac{(Mg^{++})}{(H^{+})^2} (H_4SiO_4)^2 \quad *$$

From the mass transfer diagrams for the Stoddard Mine quartzite and the Yellow Jacket skarn it can be shown that silica was removed and thus the solution was under saturated with respect to quartz.

*Parentheses indicate activity of species enclosed.

Figure 21. Mass transfer within the skarns of the Yellow Jacket Mine. Total distance between Y-21 and S-29 is 10 feet. Distance between S-29 and S-8 is 3300 feet.
Y-21 and Y-26 are limestones, (chemical analysis of these samples is listed in Table 7), Y-25 is diopside skarn, S-29 and S-8 are quartz monzonite.

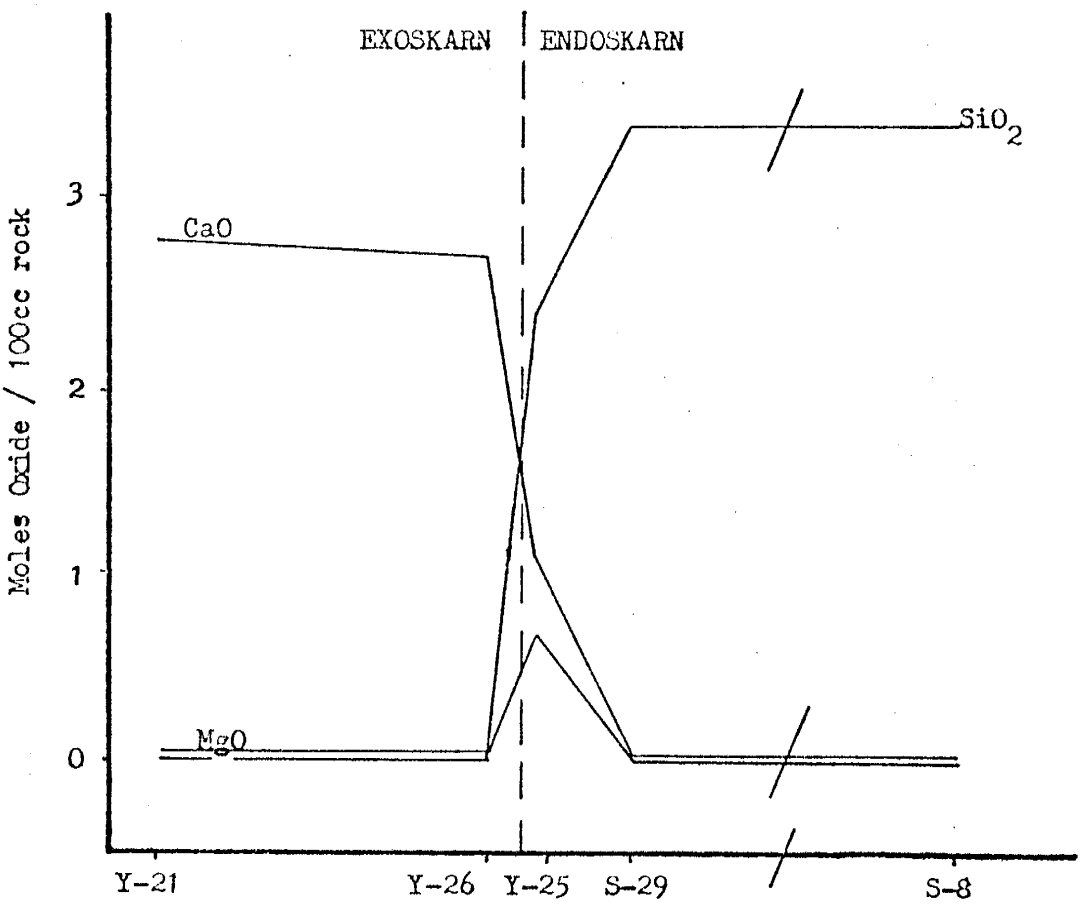
EXOSKARN
ENDOSKARN
SiO_2
CaO
MgO
Moles Oxide / 100cc rock
3
2
1
0
Y-21
Y-26
Y-25
S-29
S-8

The amount of CaO and MgO, however, increase with the formation of diopside. The conclusion derived from these facts is that the stability of diopside was dependent on the aqueous phase for the introduction of Ca^{++} and Mg^{++} but that the SiO_2 was supplied by the host. These relationships also hold true for the formation of tremolite from diopside and quartz.

Figure 22 represents the stabilities of the minerals in the system $CaO-MgO-SiO_2-H_2O-HCl$ at 250°C and 1 bar in terms of Ca^{++}, Mg^{++}, and H^+ activities, SiO_2 is conserved between phases. The presentation of the diagram as given is not strictly correct since a greater pressure is needed to maintain a liquid phase. Molar volume data for the ions at 250°C was unavailable, preventing the calculation of mineral stabilities at higher pressures. As Beane (1974) points out, however, for most solid-liquid reactions, pressure corrections on equilibrium constants are negligible in the range of a few hundred bars above unity. Therefore the diagram as drawn at one bar should change little with moderate increases in pressure. Also, in general, it can be reasonably stated that dissolved gases at these low pressures and moderate temperatures will behave approximately ideally, negating the need for fugacity coefficents.

The usefulness of the activity diagram is further enhanced by the addition of the saturation surfaces of calcite, dolomite, and magnesite. Stability fields for those minerals are not defined for the diagram because the stability fields of the phases are based upon the conservation of SiO_2 which is not contained in any of these carbonates. The dissociation of calcite is written as

$$CaCO_3 + 2H^+ = Ca^{++} + CO_2 + H_2O$$

Figure 22. The system CaO-MgO-SiO_2-H_2O-HCl at 250°C, 1 bar, in contact with a ubiquitous aqueous phase, $A_{H_2O} = 1$, SiO_2 is conserved. (Thermodynamic data and its sources are listed in Appendix B)

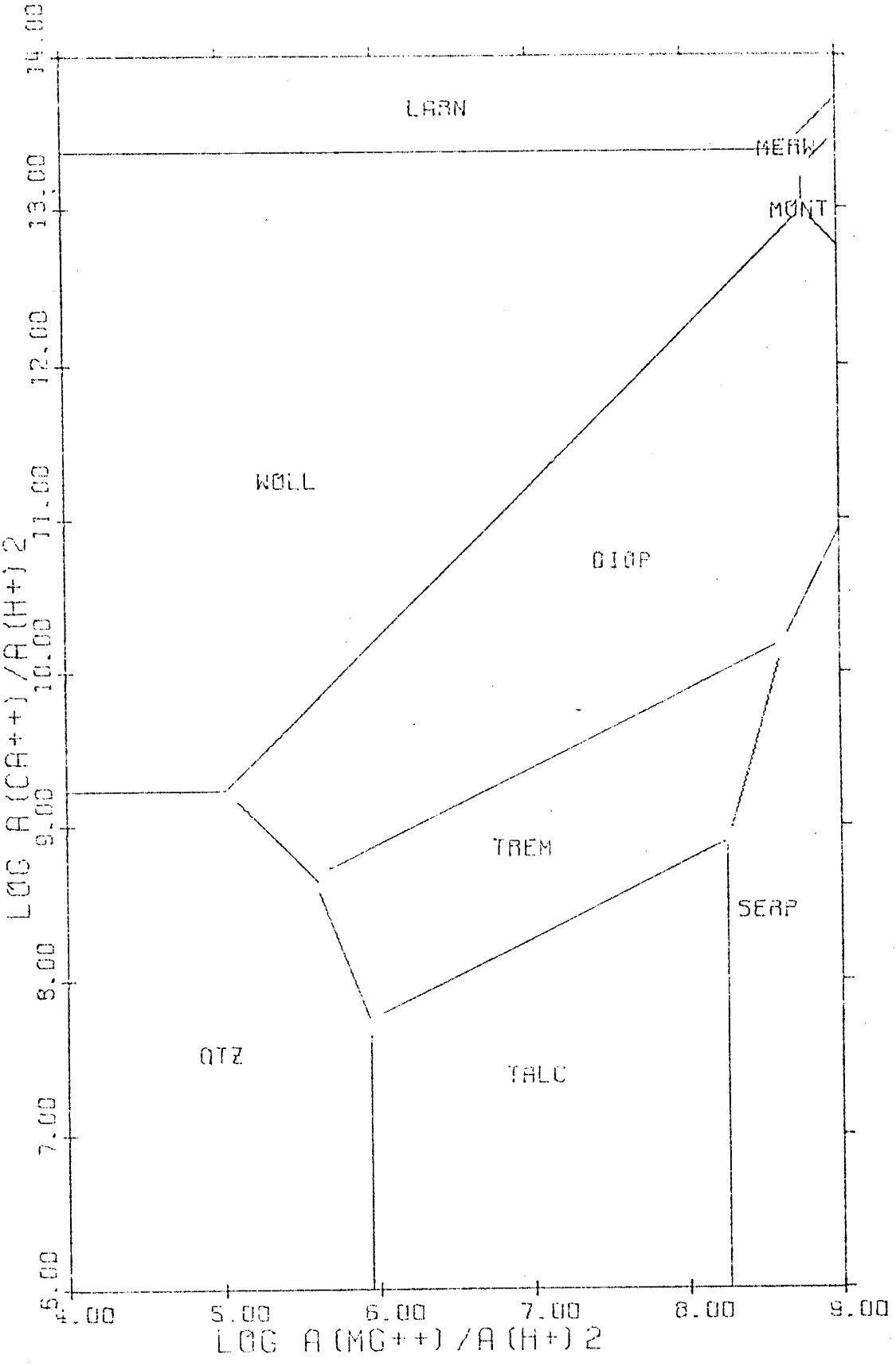
LARN
MERW
MONT
WOLL
DIOP
TREM
SERP
QTZ
TALC
14.00
13.00
12.00
11.00
10.00
9.00
8.00
7.00
6.00
4.00
5.00
6.00
7.00
8.00
9.00
LOG A(CA++)/A(H+)2
LOG A(MG++)/A(H+)2

for which

$$\log K_s = \log(Ca^{++})/(H^+)^2 + \log f_{CO_2}$$

Therefore, for a given P_{CO_2} the activity ratio determined from the equation

$$\log(Ca^{++})/(H^+)^2 = \log K_s - \log f_{CO_2}$$

represents the limiting value defined by equilibrium with respect to calcite in the system. Also, note from the relationship stated for the right side of the equation, an increasing P_{CO_2} decreases the required $(Ca^{++})/(H^+)^2$. The $(Ca^{++})/(H^+)^2$ and $(Mg^{++})/(H^+)^2$ ratios required for the saturation of the carbonate minerals at various CO_2 partial pressures have been superimposed over the silicate stability fields in Figure 23.

Consideration of the equilibrium assemblege diopside + calcite found in the Ferro Mine provides limits for the maximum possible CO_2 partial pressure in the system. The minimum log $(Ca^{++})/(H^+)^2$ ratio for diopside stability is 8.6. This value when entered into the equation for the dissociation constant of calcite, corresponds to an equilibrium CO_2 partial pressure of 1.62 atms. If the partial pressure of CO_2 should exceed this amount, the calcium to hydrogen ratio would be held to a value less than that necessary for diopside stability relative to tremolite.

A saturation surface for anhydrite may be calculated in a similar manner. However, the dissociation of anhydrite,

$$CaSO_4 = Ca^{++} + SO_4^{=}$$

is independent of the activity of hydrogen. Because the axis of the activity diagram is expressed in terms of the ratio of the activities of calcium and hydrogen, the calcium activity of the anhydrite

Figure 23. The system $CaO-MgO-SiO_2-CO_2-H_2O-HCl$ at 250°C, 1 bar, in contact with a ubiquitous aqueous phase, $A_{H_2O} = 1$. SiO_2 is conserved and f_{CO_2} is contoured.

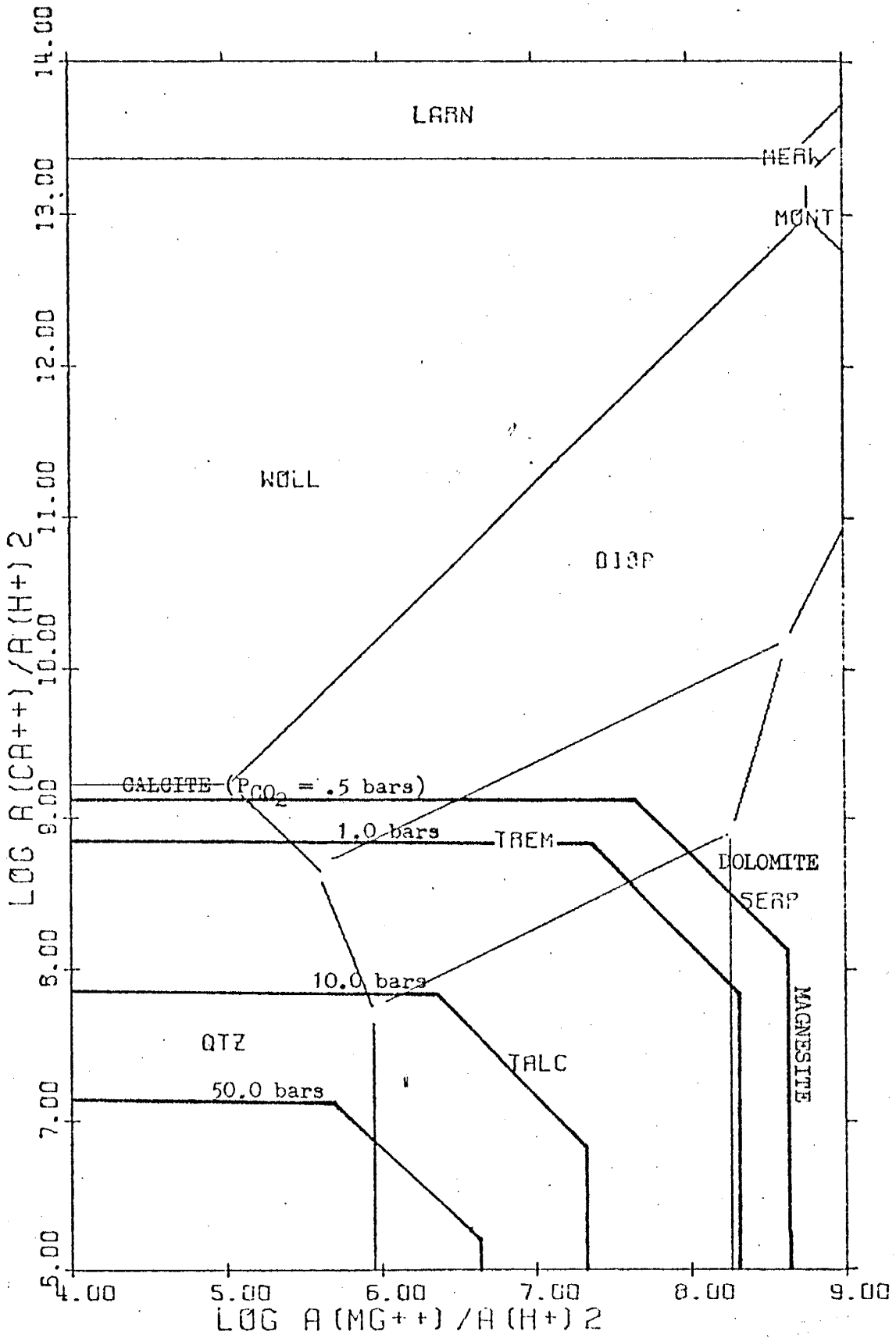
LARN
HERL
MONT
WOLL
DIOP
CALCITE (P_{CO_2} = .5 bars)
1.0 bars
TREM
DOLOMITE
SERP
10.0 bars
QTZ
TALC
50.0 bars
MAGNESITE
14.00
13.00
12.00
11.00
10.00
9.00
8.00
7.00
6.00
5.00
4.00
5.00
6.00
7.00
8.00
9.00
LOG A(CA++)/A(H+)2
LOG A(MG++)/A(H+)2

dissociation must be converted to this activity ratio. This conversion is accomplished by adding hydrogen to both sides of the dissociation reaction; which has no effect on log K_s for anhydrite. The equation then becomes,

$$CaSO_4 + 2H^+ = Ca^{++} + 2H^+ + SO_4^=$$

for which

$$\log K_s = \log(Ca^{++})/(H^+)^2 + \log(H^+)^2 \times (SO_4^=)$$

Figure 24 is a plot of $\log(SO_4^=)$ versus $\log(Ca^{++})/(H^+)^2$ for various pH values according to the above equation at 250°C. It should be apparent from this diagram that for the $(Ca^{++})/(H^+)^2$ ratio to reach the minimum required for diopside stability, (dashed line), the sulfate activity must be extremely small or the pH very high.

Anhydrite rather than gypsum was used as the $CaSO_4$ phase above because gypsum dehydrates to anhydrite at temperatures above 50°C. One important aspect of this dehydration is the effect which it has on porosity. The molar volume of $CaSO_4 \cdot 2H_2O$ is 74.69cc as compared to 45.94cc for $CaSO_4$. Therefore, a unit of gypsum with no porosity, lying between two rigid rock units, will obtain a porosity of 38% upon conversion to anhydrite.

In previous discussions on the geology of the contact deposits, gypsum was almost always present in the area. Because the temperature during the mineralization was shown to be about 250°C, it would seem probable that these nearby gypsum beds would obtain a temperature of at least 50°C and therefore would have altered to beds of anhydrite with high porosity. If the porosity developed was maintained open the difference in hydrostatic head between this zone and the surrounding rock would funnel the surrounding groundwaters into the rock until

Figure 24. Anhydrite equilibrium in terms of $(Ca^{++})/(H^{+})^2$ and $(SO_4^{=})$ at various pH values, 250°C, 1 atm., $A_{H_2O} = 1$, and in the presence of quartz.

Dashed line D corresponds with the minimum value of $(Ca^{++})/(H^{+})^2$ at which diopside can be stable.

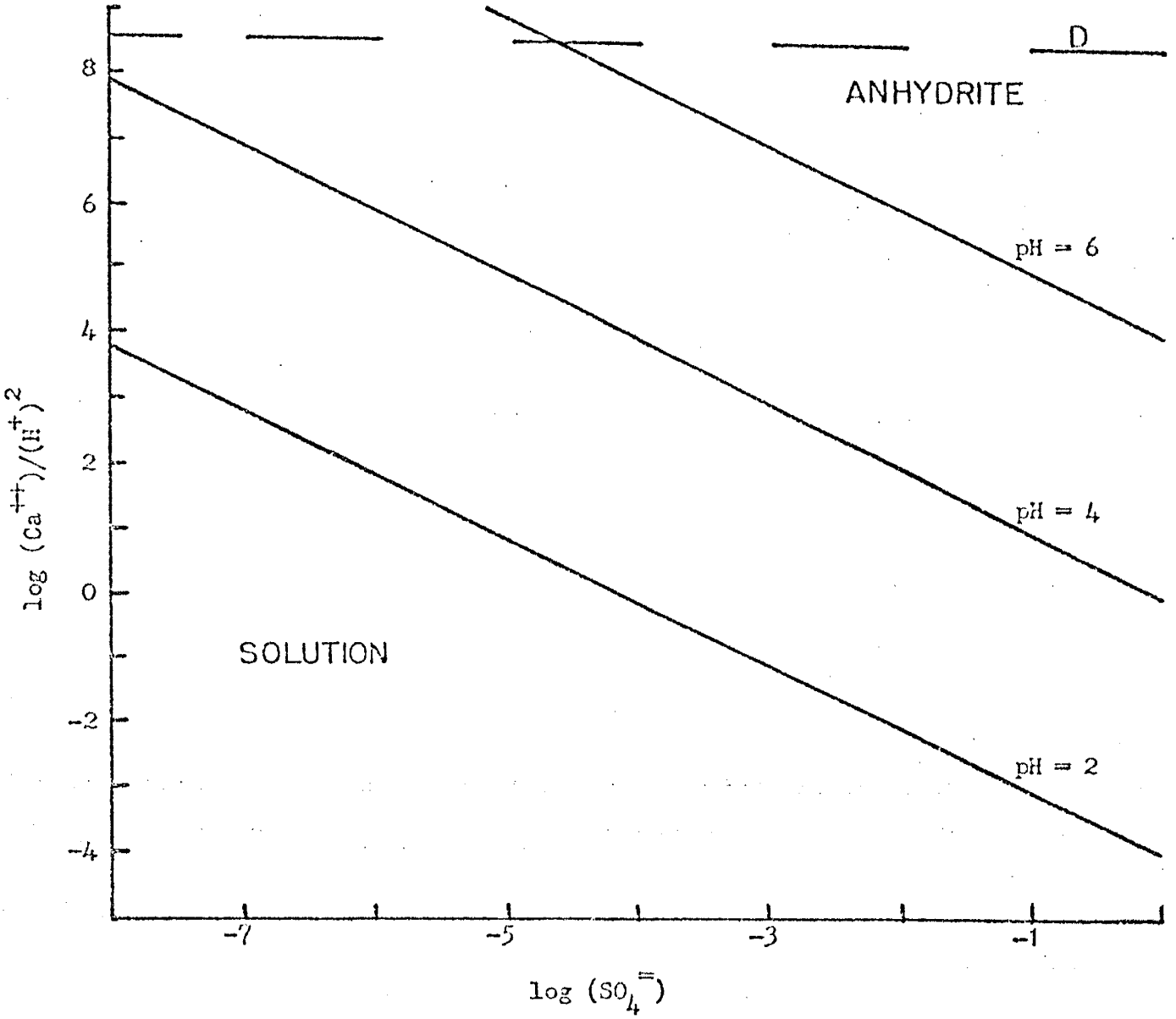
D
ANHYDRITE
pH = 6
pH = 4
pH = 2
SOLUTION
8
6
4
2
0
-2
-4
-7
-5
-3
-1
log $(Ca^{++})/(H^{+})^2$
log $(SO_4^{=})$

the pressures had equalized. Water released by the dehydration of gypsum, however, fills this pore space, thus maintaining a balanced hydrostatic head relative to the surrounding rocks. Yet heating the country rock to form anhydrite from gypsum also increases the temperature of the groundwater which decreases its density. This newly created low density water attempts to displace the overlying cooler, denser water initiating a flow through the area.

Figure 25 is a hypothetical case of an intrusive cutting through interbedded gypsum and limestone. The gypsum units near the pluton have dehydrated to anhydrite, causing the flow lines to converge upon this zone of low resistance. The flow is maintained by heating the water as it approaches the intrusion, thus lowering its density, which in turn causes it to rise.

Alteration of the Lone Mountain Laccolith

Earlier in the paper it was noted that the laccolith showed a general spatial zoning of mafic minerals in which biotite was centrally located with a peripherial zone of diopside-bearing rock. The zoning of the stock might be explained in terms of the cooling history of the intrusion. If the magma initially crystallized pyroxene and was intruded at high temperatures into a cool country rock, the periphery of the melt might crystallize quickly enough to prevent further interaction of the melt and the pyroxene. The core of the melt, however, would cool much slower, allowing the pyroxene to react with the melt, continuously forming lower temperature phases and eventually biotite. While this may explain the zoning, it does not agree with the observed destruction of biotite by diopside. It is very difficult to explain the reaction, biotite → diopside in terms of a magmatic

Figure 25. Groundwater flow lines converging on an anhydrite unit near an intrusive. Porosity of the anhydrite >> porosity of the gypsum and limestone.

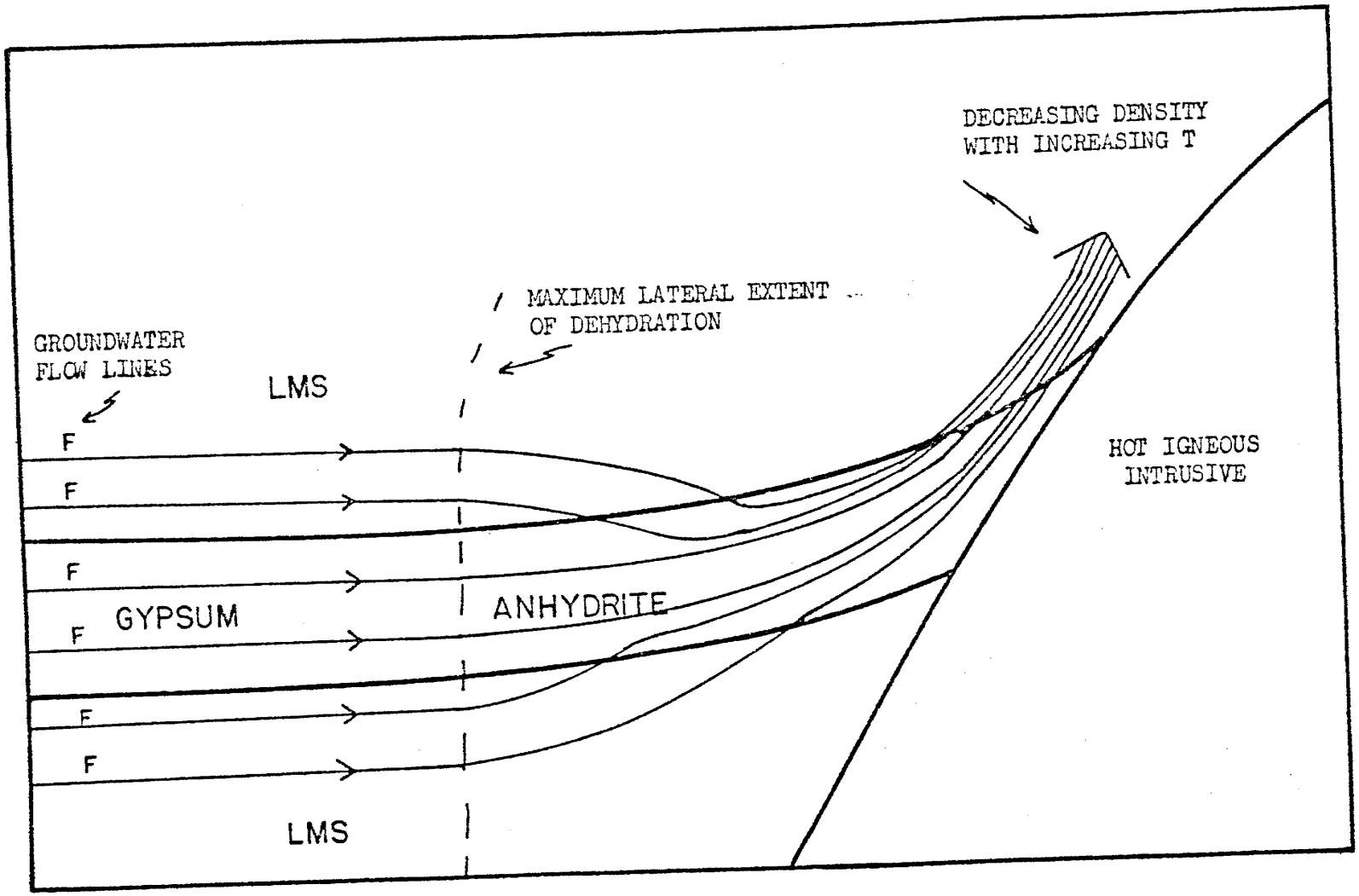
DECREASING DENSITY
WITH INCREASING T
MAXIMUM LATERAL EXTENT
OF DEHYDRATION
GROUNDWATER
FLOW LINES
LMS
F
F
F
F
F
F
F
GYPSUM
ANHYDRITE
LMS
HOT IGNEOUS
INTRUSIVE

process because in terms of Bowen's reaction series diopside in the skarns (both endo- and exoskarns), and as thick veins within the laccolith, it is suggested that the diopside in the quartz monzonite is of hydrothermal origin. The biotites are very light brown with maximum absorption in planar light, indicating a magnesium biotite. Therefore the Mg-conserving reaction for the replacement of biotite by diopside is postulated to be

$$KMg_3AlSi_3O_{10}(OH)_2 + 3H_4SiO_4 + 3Ca^{++} = 3CaMgSi_2O_6 + K^+ + Al^{+3} + 2H^+ + 6H_2O$$

Because there is no method by which the temperature and aqueous solution composition could be determined, a strict thermodynamic treatment of the process could not be presented.

It was also noted that the antiperthite exhibited corroded edges, possibly indicating some form of hydrothermal attack. While antiperthite may form from the crystallization of a sodium rich melt, there is also the possibility that the albite of the antiperthite is the result of hydrothermal action on K-feldspar, by the reaction

$$KAlSi_3O_8 + Na^+ = NaAlSi_3O_8 + K^+$$

for which

$$\log K = \log(K^+)/(Na^+)$$

Figure 26 is a plot of the equilibrium curve for orthoclase + albite in terms of $\log(K^+)/(Na^+)$ versus temperature at 140 bars. The dashed line in Figure 26 corresponds to the ratio of molarities of potassium to sodium for the Carrizozo municipal water well 6 miles south of Lone Mountain, (New Mexico Quality Control Commission, 1975). For a first approximation it will be assumed that the ratio of molarities is equal to the ratio of activities. From this diagram it can be

Figure 26. Equilibrium phase boundry for albite + microcline at 140 bars, (H. Helgeson, personal communication, 1976)

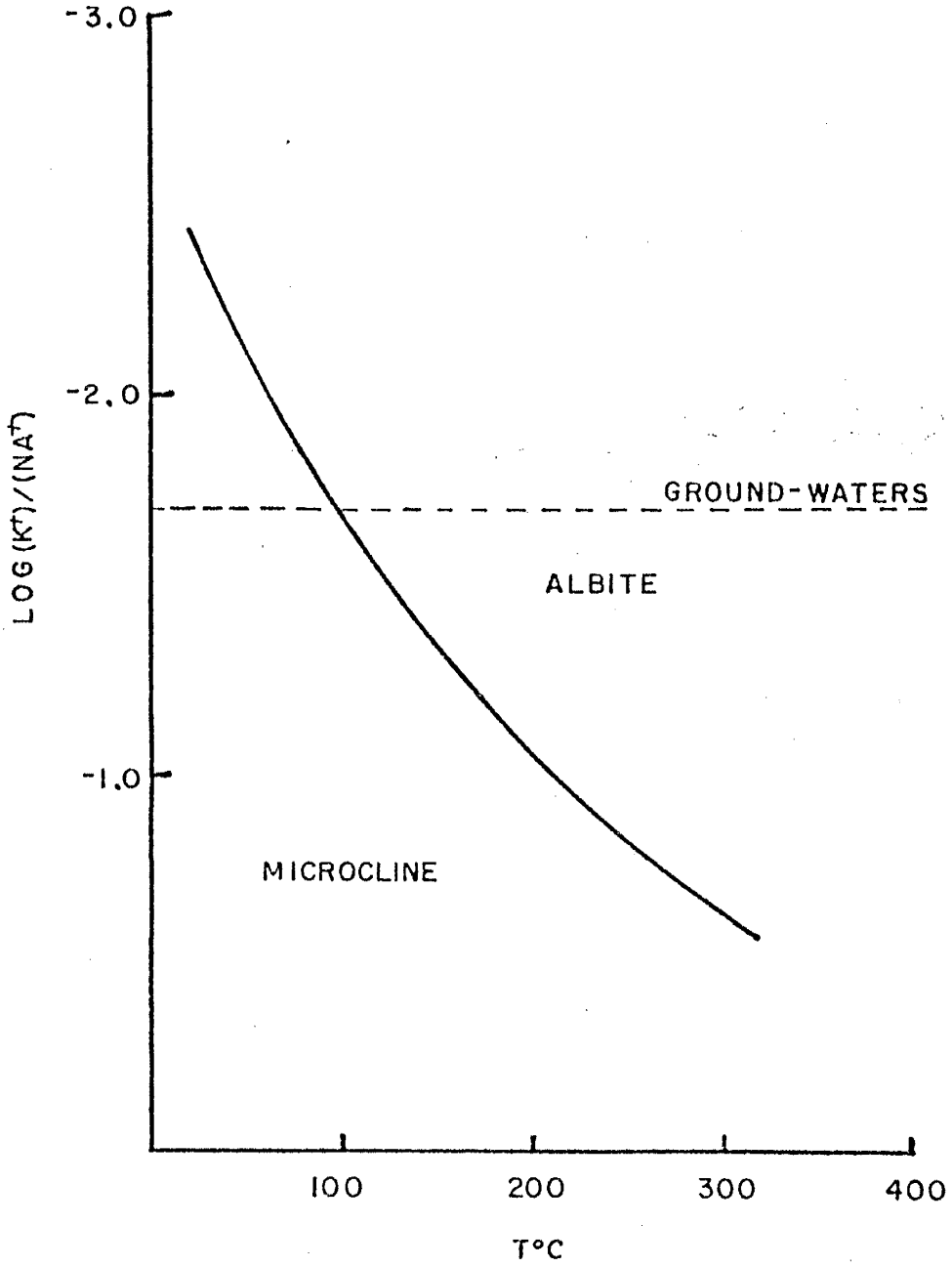
-3.0
-2.0
-1.0
LOG(K+)/(NA+)
GROUND-WATERS
ALBITE
MICROCLINE
100
200
300
400
T°C

shown that if the waters had flowed through the laccolith as postulated above, and if the temperature remained above 100°C, the K-feldspar within the laccolith would have been albitized until the K/Na ratio had been shifted according to the reaction to the value corresponding to equilibrium.

Stability of the Iron Oxide Minerals

In addition to the Ca-Mg silicates and carbonates the skarns also contain large amounts of iron oxides. The following will briefly describe the behavior of iron in a hydrothermal system as outlined by Beane and Titus (1973).

Earlier in the paper it was shown that magnetite and hematite are normally found coexisting within the iron ores. The equilibrium between magnetite and hematite can be expressed as

$$2Fe_3O_4 + \tfrac{1}{2}O_2 = 3Fe_2O_3$$

Figure 27 is a plot of the equilibrium curve for hematite and magnetite in terms of the oxygen fugacity and temperature. At 250°C the oxygen fugacity is fixed at 10^{-32} atm. by the coexistence of magnetite and hematite.

The equilibrium constants for the dissolution of magnetite and hematite decrease with increasing temperature. However, as temperature rises above 150°C the total amount of iron in a solution coexisting in equilibrium with these two oxides increases owing to the formation of iron hydroxide complexes, (Beane and Titus, 1973). The most stable aqueous iron species at low temperatures are the free ions. With increasing temperatures ferric and ferrous hydroxide complexes become increasingly stable, and above approximately 150°C they become the dominate aqueous iron species, (Table 8). Assuming for simplicity

Figure 27. Equilibrium phase boundry for magnetite + hematite. (Beane and Titus, 1973).

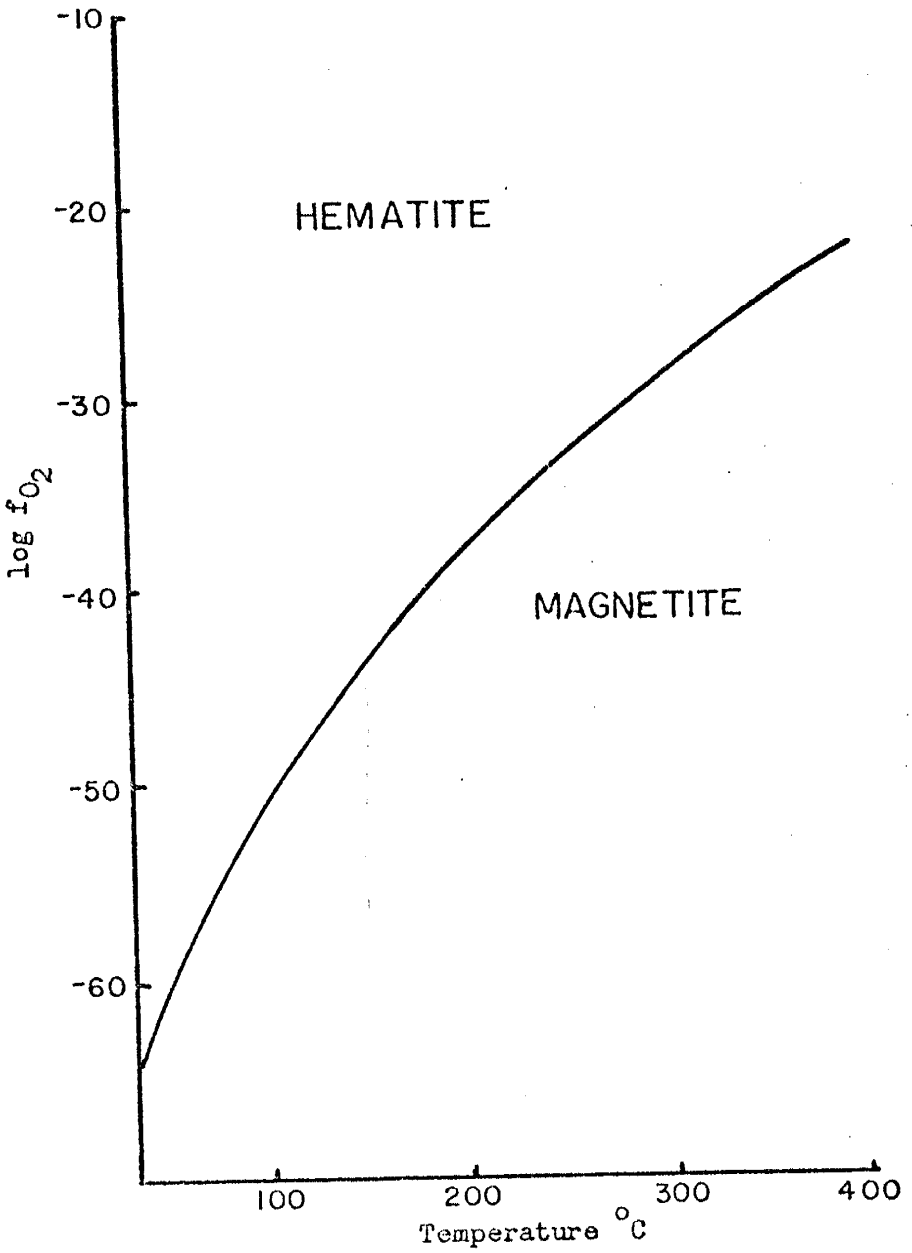
-10
-20
-30
-40
-50
-60
HEMATITE
MAGNETITE
log f_{O_2}
100
200
300
400
Temperature °C

Table 8. The dominant aqueous iron species at various temperatures and pH values, (Beane and Titus, 1973).

$T^{\circ}C$	25	100	150	200	250	300
pH	2-6	2-6	2-6	2-6	2-6	2-6
Fe^{+2}	X-X	X-X	---	---	---	---
Fe^{+3}	---	---	---	---	---	---
$FeOH^{+2}$	---	X--	X--	X--	X--	X--
$Fe(OH)_2^{+}$	---	--X	--X	X--	X--	X--
$Fe(OH)_4^{-}$	---	--X	--X	--X	--X	--X
$Fe(OH)^{+}$	---	---	---	---	---	---

that activity equals molality, the total molality of iron in the aqueous solution coexisting with magnetite and hematite can be calculated by adding the activities of iron contributed by each aqueous iron species at a specified pH. Figure 28 shows how the total concentration of iron varies with temperature at a constant pH in a solution in equilibrium with magnetite + hematite.

From the relationships exhibited in Figure 28 it is apparent that the precipitation of iron oxides from a saturated solution can be promoted by several means. The solubility of magnetite + hematite obtains a minimum value at temperatures of approximately 100 - 150°C. Should an iron saturated aqueous solution be heated from a lower temperature or cooled from a higher temperature, magnetite and hematite would precipitate to maintain equilibrium. However, as shown earlier, the deposits at Lone Mountain are replacement deposits limited to limestone units. Deposition of magnetite and hematite resulting from a changing temperature fails to explain this limitation of host rocks. In addition, temperature variation fails to accomodate the dissolution of calcite at the depositional site, as the rise in pH resulting from the decreasing concentration of iron would favor calcite stability.

Magnetite and hematite may also be precipitated from an aqueous solution at a constant temperature and pressure in response to a change in pH. At Lone Mountain the dissolution of the limestone host would consume two moles of hydrogen ion for every mole of calcite destroyed.

$$CaCO_3 + 2H^+ = Ca^{++} + H_2O + CO_2$$

From Figure 28 it is shown that if an iron saturated aqueous solution at a pH of 2 and 250°C reacts with a limestone the resulting increase in pH up to about 4 would decrease the solubility of iron thus

Figure 28. Solubility of iron with respect to temperature and pH, (Beane and Titus, 1973).

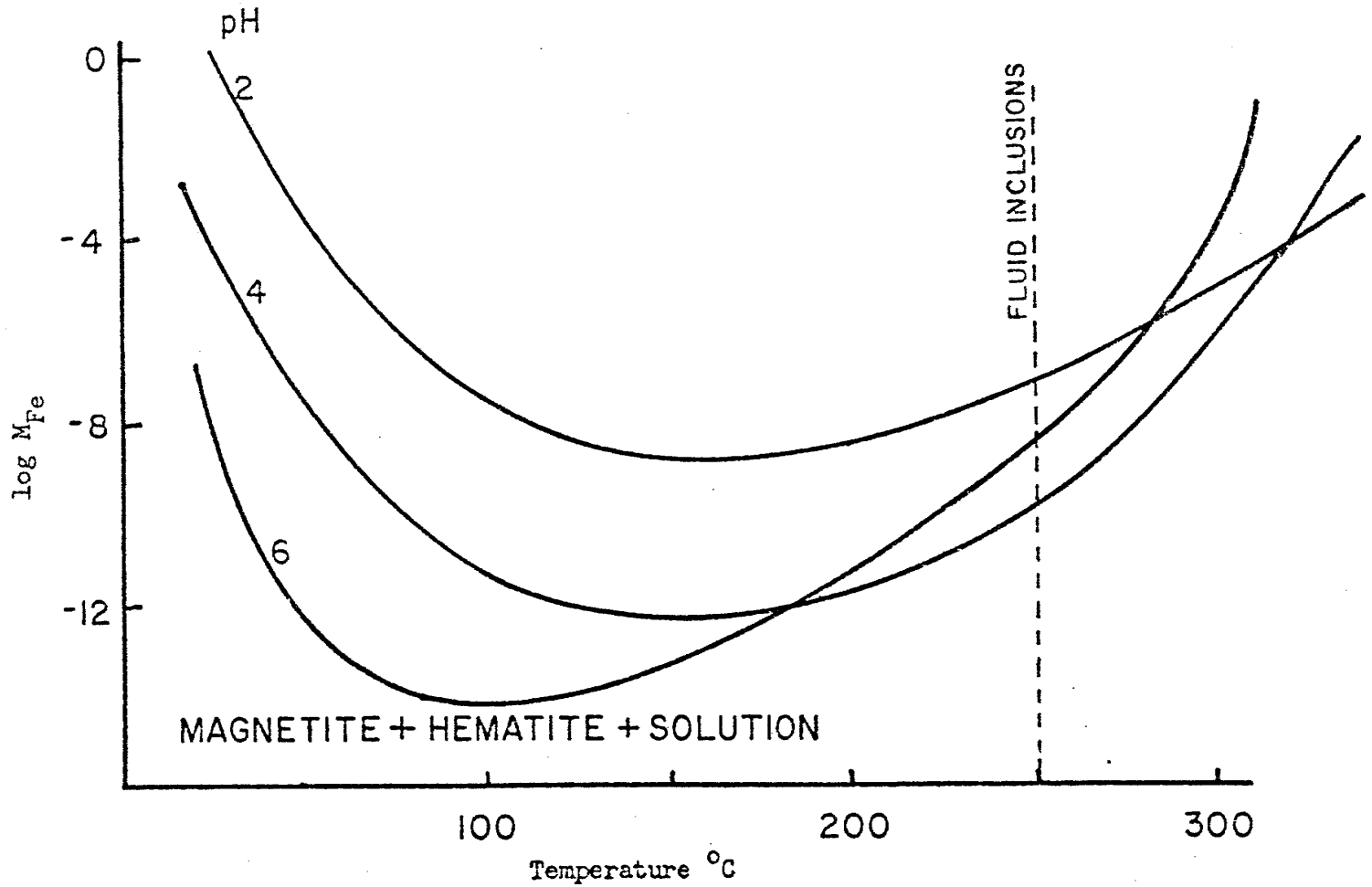
pH
0
-4
-8
-12
log M_{Fe}
2
4
6
FLUID INCLUSIONS
MAGNETITE + HEMATITE + SOLUTION
100
200
300
Temperature °C

precipitating small amounts of the iron oxides.

The amount of iron deposited from a liter of solution is very small. In figure 28 it is shown that at 250°C, a change in pH from 2 to 4 would result in the maximum amount of iron being precipitated as magnetite and hematite, which amounts to only 1.0×10^{-8} moles of Fe or 10^{-6} grams of hematite. Therefore in order to deposit the 20,000 tons of iron ore removed from the Yellow Jacket Mine alone, (Griswold, 1959), 10^{13} liters of watet must move through the system.

As shown in a hypothetical case earlier, the presence of gypsum beds in the sedimentary section can greatly enhance the flow of water near an intrusive. The presence of gypsum adjacent to each of the large iron deposits and the large volumes of water necessary to deposit large amounts of iron suggests that the gypsum has played an important role in the deposition of the iron deposits at Lone Mountain despite the fact that gypsum is chemically inactive in the depositional environment.

SUMMARY AND CONCLUSIONS

The Lone Mountain intrusive is one of at least ten Tertiary stocks and laccoliths occurring in the region between Corona and Ruidoso, at the approximate intersection of two major structural features, the Capitan Lineamint and the Mescalero Arch.

The main mass of Lone Mountain consists of a quartz monzonite intrusive drapped by steeply dipping beds of the Permian San Andres Formation. Both the intrusive and the San Andres Formation are overlain unconformably by a Tertiary(?) agglomerate in the southwest corner of the study area. Several quartz monzonite dikes are found cutting through both the stock and the San Andres limestones. The dikes typically display a 1-2 inch chill margin where they are found emplaced in sedimentary rocks, yet display no such margins where they cut through the stock, indicating that they were probably intruded while the stock was still hot.

Evidence was found which suggests that the stock may have originally had a more granitic composition, (ie. a larger K-feldspar component), but owing to the introduction of sodium rich solutions which reacted with the K-feldspar to form albite at subsolidus temperatures, the rock has obtained a normative composition of quartz monzonite.

Contact metamorphism is restricted primarily to several large roof pendants composed of blocks of the San Andres Formation. Metamorphism of sedimentary rocks adjacent to the outer perimeter of the stock is very rare and is usually associated with one of the dikes. Geometric relationships within the largest iron deposit at the Yellow Jacket Mine also indicate that the metamorphism is most pervasive in the vicinity of the dikes nearest the sedimentary-

stock contact. Apparently, the dike and the stock singularly were not able to supply the necessary heat for pervasive metamorphism. However, the combined effects of the dikes and stock were enough to produce sufficient temperatures for a sufficient length of time to result in the deposition of large amounts of magnetite and hematite, and a number of silicate minerals.

The contact metamorphism occurs primarily in limestone units of the Permian San Andres Formation. The deposition of silicate minerals, however, is limited to quartzite units, (exoskarn), and to thin zones within the periphery of the stock and dikes, (endoskarn). The presence of this endoskarn, though limited, is highly significant in that it indicates that neither of these intrusives could be the source of the hydrothermal solutions because late stage magmatic fluids would be low in Ca^{++} necessary for diopside deposition, (Burnham, 1967). Also, the observed replacement of biotite by diopside within the laccolith is very difficult to adequately explain in terms of a magmatic process. Therefore, the hydrothermal solutions once active at Lone Mountain are felt to have been local ground waters, drawn towards the laccolith by a heat driven convection cell. Though these solutions were in equilibrium with the host rocks at ambient temperatures, the heat from the dikes and stock moved the system into disequilibrium, resulting in the formation of a new suite of minerals.

The composition of the aqueous solutions responsible for the mineralization at Lone Mountain can now be presented in light of the discussions on mineral stabilities and the geologic and mineralogic data presented earlier in this paper. These conclusions are based upon

thermodynamic data available at the time this paper was compiled. Future refinement of this data may show the calculations presented to be in error with respect to absolute dimensions but not in terms of the process.

As an aqueous solution containing free ions of iron is heated, the hydroxide complexes of iron become increasingly stable. At 250°C the dominant aqueous iron species are $Fe(OH)_2^+$ and $Fe(OH)_4^-$. The hydroxyl components of these complexes are obtained from the dissociation of water;

$$H_2O = H^+ + OH^-$$

Therefore for every mole of $Fe(OH)_2^+$ that forms from free ions of iron upon raising the temperature, 2 moles of water are destroyed which in turn liberates 2 moles of hydrogen ion into the aqueous solution. Similarly, for one mole of $Fe(OH)_4^-$ created, 4 moles of hydrogen are placed into solution. If the solution originally contained only 0.5 ppm Fe and if all this iron went into $Fe(OH)_2^+$ complexes, $10^{-4.7}$ moles of hydrogen would be placed into solution, which would then have a pH of 4.7. If the formation of $Fe(OH)_4^-$ complexes is considered the pH would be even lower, 4.4. Therefore, as the ground waters near Lone Mountain were heated to the 250°C determined for the skarns, the solutions became increasingly acidic by the hydrolysis of dissolved iron.

Earlier it was shown that to obtain diopside stability the sulfate activity had to be very small or the pH had to be very high. As we have just seen, the pH of the solutions was probably relatively low, and because there are large amounts of diopside in the skarns, the sulfate activity had to be very low in order to satisfy the $(Ca^{++})/(H^+)^2$

requirements for silicate stability. The abundance of gypsum in the area of Lone Mountain has resulted in groundwaters high in sulfate. However, with increasing temperatures, anhydrite becomes increasingly insoluble; thus increasing amounts of sulfate are removed from solution as the temperature rises at anhydrite saturation. Such precipitation of anhydrite would also lower the activity of calcium, pushing the $(Ca^{++})/(H^{+})^2$ ratio away from the value needed for diopside stability. On the other hand, if the solution is saturated with anhydrite at a constant T and P the sulfate activity will decrease if calcium is added to the system. As the hydrothermal solutions approached the intrusive they are likely to have become increasingly acidic, owing to the complexing of iron with (OH^{-}). Small amounts of acid attacked the limestones, liberating calcium and CO_2. The calcium then precipitated out the sulfate in solution as anhydrite, (ie. the patches of selenite crystals adjacent to the Ferro Mine ore body). Continued dissolution of the limestone added calcium to the solution and increased both the pH and the $(Ca^{++})/(H^{+})^2$ to stabilize diopside.

Saturation in the aqueous phase with respect to calcite will also prevent the ratio $(Ca^{++})/(H^{+})^2$ from reaching the value needed for diopside saturation if the P_{CO_2} is greater than 1.62 atms. at 250°C. Therefore in order to have deposited the diopside in the skarns at Lone Mountain the mineralizing solutions must have maintained a CO_2 partial pressure of less than 1.62 which indicates that the system was open or was mixed volatile. The removal of the CO_2 gas generated by the dissolution of limestone was necessary, because if $P_{CO_2} = P_{total}$, then the CO_2 building up in the system, (closed system), would have allowed calcite to saturate at a $(Ca^{++})/(H^{+})^2$ value significantly

less than that required for diopside saturation as shown by Figure 25.

Earlier in the paper it was shown that the magnetite veins of the Stoddard Mine graded laterally into limestone. As the dissolution of calcite raises the pH by consuming acid, the solubility of iron in the aqueous solution decreases up to a pH of about 4 at 250°C. Once the solution reaches the saturation of magnetite and hematite, the dissolution of small amounts of calcite will initiate a reciprocal precipitation of magnetite and hematite,

$$2Fe(OH)_2^+ + CaCO_3 = Fe_2O_3 + CO_2 + Ca^{++}$$

or

$$2Fe^{+3} + 3CaCO_3 = Fe_2O_3 + 3CO_2 + 3Ca^{++}$$

thereby slowly replacing the limestone unit. Dehydration of gypsum beds within the areas of mineralization results in the introduction of huge volumes of water passing through a relatively small area. Even though the amount of iron contributed by each liter of solution is very small, the availability of vast quantities of water results in the formation of large deposits.

At this point, with the addition of Ca^{++} and the increased pH from calcite dissolution at CO_2 partial pressures of less than 1.6 atms., the $(Ca^{++})/(H^+)^2$ ratio is large enough for diopside saturation. Little can be said of the $(Mg^{++})/(H^+)^2$ ratio except that because diopside is found in the skarns and magnesite is not, the value for the ratio must have been less than that needed for magnesite stability at low CO_2 partial pressures, (less than approximately 8.0) and yet greater than 5.0 in order to saturate with diopside.

Thus far, however, diopside stabilities have been discussed in terms of (Ca^{++}), (Mg^{++}), and pH, ignoring the SiO_2 component. Diopside

was observed to form almost exclusively within the igneous rocks and quartzites. The solutions and the limestones were apparently unable to furnish the needed silica for diopside saturation. The quartz monzonite stock and the quartzite beds however, contained an excess amount of silica in relation to the amount needed to form a diopside rock. Small amounts of SiO_2 were dissolved and carried away by the solutions but for the most part the silica remained in the rock, forming diopside.

Late stage tremolite may be the result of one of the two following processes. First, low temperatures favor the formation of amphiboles, (tremolite), over the pyroxenes, (diopside). Therefore, the tremolite may be the result of decreasing temperatures during the latter stages of the metasomatism. Or secondly, near the end of the metasomatism, the amount of calcite being dissolved began to drop off as the limestone beds were almost totally replaced by iron oxides. The pH and (Ca^{++}), at a given point in space, slowly decreased, moving the solution into the tremolite stability field.

Appendix A: Calculation of normative rock compositions

The standard Niggli and CIPW norms long used by igneous petrologists to classify fine grained igneous rocks are based upon a step-wise distribution of major element oxide components, obtained through whole rock chemical analysis, among standard sets of minerals with ideal stoichiometric compositions. Though this method proves to be satisfactory in comparing one igneous rock to another, it gives a distorted representation of the mineralogic composition of the rock for the following reasons. First, the minerals among which the oxide components are distributed need not represent the true mineralogy of the rock. Second, even if a representative set of minerals is used, no allowance may be made for minerals which in reality have non-ideal compositions owing to solid solutions or ion substitution. Third, being a step-wise calculation, if one of the oxide weight percent values is in error because of an imprecision of the analytical method, then this error will be passed along totally to the last mineral in the calculation which contains the errant oxide component.

Because of the above deficiencies, the use of these normative compositions in the thermodynamic prediction of solution-rock interactions would necessarily give erroneous results relative to the actual process. However, it is possible to closely approximate the true rock composition by simultaneously distributing the oxide components, (determined through whole rock analysis), among the actual minerals and mineral compositions found in the rock. The calculations are based upon the simultaneous solution of a set of linear equations in the form

$$A_1X + B_1Y = K_1$$
$$A_2X + B_2Y = K_2$$

for which, K_1 and K_2 are the number of moles of oxides contained in a 100 gram sample of rock; X and Y are the calculated number of moles of minerals A and B in the sample; coefficents A_1 and A_2 are the number of moles of oxides K_1 and K_2, respectively, contained in one mole of mineral A. Thus, X and Y are the unknown variables related to K_1 and K_2 by the constants A_1, B_1, etc.

Figure 29 is a sample set of equations for a rock containing six minerals and also which has been analyzed for the seven major elements. Note that a biotite composition lying halfway between annite and phlogopite has been used to demonstrate the ability of this method of calculating norms to use a variety of mineral compositions. The results of a chemical analysis are normally presented as weight percent of the oxides. However, as the terms of the left side of the equations are given as moles, these values must be converted to moles before the computation may be performed. As weight percent is equivalent to grams per 100 gram sample, the weight percent values are equivalent to the number of grams of each oxide if a 100 gram sample size is assumed. This value when divided by the molecular weight of the oxide then yields the number of moles of the oxide in a 100 gram sample of the rock. The computed values for the unknown variables are thus in terms of the number of moles of each mineral per 100 grams of rock. The volume contribution of each mineral is then determined by multiplying the number of moles of a mineral by its molar volume. It is then a simple matter to calculate the volume percentage of each mineral in the original sample.

Because the actual mineral assemblage and mineral compositions are used in this calculation and because errors in the chemical analysis

Appendix A (Figure 29). Sample set of linear equations used to calculate a normative rock composition.

	QUARTZ	K-SPAR	ALBITE	ANORTHITE	MAGNETITE	BIOTITE	WT. % OF OXIDES
SiO_2	1xQ +	3xK +	3xAb +	2xA +	0 +	3xB	= 60
Al_2O_3	0 +	.5xK +	.5xAb +	1xA +	0 +	.5xB	= 10
FeO	0 +	0 +	0 +	0 +	3xM +	1.5xB	= 3
MgO	0 +	0 +	0 +	0 +	0 +	1.5xB	= 2
Na_2O	0 +	0 +	.5xAb +	0 +	0 +	0	= 8
K_2O	0 +	.5xK +	0 +	0 +	0 +	.5xB	= 9
CaO	0 +	0 +	0 +	1xA +	0 +	0	= 8

are distributed evenly among the minerals this method results in a rock composition which closely approximates the true composition of the sample. Also, this method can easily be applied to any group of rocks, sedimentary, metamorphic, or igneous, as the unknown variables are based only on the mineralogy of the rock.

Appendix B. Thermodynamic data for phases in the system CaO-MgO-SiO_2-H_2O-CO_2.

Name	Formula	$S^{o}_{298.15}$ [a] cal/mole-deg	H_f^{o} [a] cal/mole
Quartz	SiO_2	9.88	-217650..
H_2O (liq)	H_2O	16.71	-68315..
CO_2 (gas)	CO_2	51.06	-94051.
Calcite	$CaCO_3$	22.15	-288592.
Magnesite	$MgCO_3$	15.70	-266081.
Dolomite	$CaMg(CO_3)_2$	37.09	-557613.
Wollastonite	$CaSiO_3$	19.60	-390640.
Larnite	Ca_2SiO_4	30.50	-551420.
Monticellite	$CaMgSiO_4$	24.50	-540800.
Diopside	$CaMgSi_2O_6$	34.20	-767390.
Merwinite	$Ca_3MgSi_2O_8$	60.5	-1091490.
Talc	$Mg_3Si_4O_{10}(OH)_2$	62.34	-1415700.[b]
Serpentine	$Mg_3Si_2O_5(OH)_4$	53.2	-1043050.
Tremolite	$Ca_2Mg_5\ Si_8O_{22}(OH)_2$	131.19	-2952935.

Appendix B, cont.

	V^{o} [a]	$C_p = a + bT + c/T^2$			
Name	cm^3/mole	a	$bx10^{-3}$	$cx10^{5}$	Source
Quartz	22.688	11.22	8.20	-2.70	c
H_2O (liq)	18.069	18.04	0	0	c
CO_2 (gas)	24465.	10.57	2.10	-2.06	c
Calcite	36.934	24.98	5.24	-6.20	c
Magnesite	28.018	18.62	13.8	-4.16	c
Dolomite	64.34	42.76	20.85	-11.53	b
Wollastonite	39.93	26.64	3.60	-6.52	c
Larnite	51.60	34.87	9.74	-6.26	c
Monticellite	51.36	34.65	6.08	-8.12	b
Diopside	66.09	52.87	7.84	-15.74	c
Merwinite	104.4	73.06	12.38	-14.81	c
Talc	136.25	84.6	41.66	-17.99	b
Serpentine	108.5	75.82	31.60	-17.58	d
Tremolite	272.92	188.07	59.36	-45.90	b

Appendix B, cont.

Sources of Thermodynamic Data

[a]Robie and Waldbaum (1968)

[b]Schnake (1977)

[c]Kelley (1960)

[d]King et al. (1967)

REFERENCES

Allmendinger, R., 1976, A model for ore genesis in the Hansonberg Mining District, Socorro County, New Mexico: unpublished Ph.D. thesis, N. Mex. Inst. of Min. and Tech.

Beane, R.E., 1974, Biotite stability in the porphyry copper environment: Econ. Geol., v. 69, pp 241-256.

Beane, R.E. and Titus, F.B., Jr., 1973, Thermal control of magnetite deposition in central New Mexico: presented 1973 Annual Meeting, G.S.A.

Burnham, C.W., 1967, Hydrothermal fluids at the magmatic stage, in Barnes, H.L., ed., Geochemistry of hydrothermal are deposits: New York, Holt, Rinehart, and Winston, Inc., pp 34-76.

Butler, Patrick, Jr., 1964, Magnetite from intrusives and associated contact deposits, Lincoln County, New Mexico: unpublished Master's thesis, N. Mex. Inst. of Min. and Tech.

Griswold, G.B., 1959, Mineral deposits of Lincoln County, New Mexico: N. Mex. Inst. of Min. and Tech., State Bur. of Mines and Min. Res. Bull. 67, 112 pp.

Kelley, K.K., 1960, Contributions to the data on theoretical metallurgy, XIII. High-temperature heat content, heat capacity, and entropy data for the elements and inorganic compounds: U.S. Bur. Mines Bull. 584, 232 pp.

Kelley, V.C., 1949, Geology and economics of New Mexico iron-ore deposits: Univ. N. Mex. Pub. in Geology, no. 2, 246 pp.

Kelley, V.C. and Silver, Coswell, 1952, Geology of the Caballos Mountains, with special reference to regional stratigraphy and structure, and mineral resources, including oil and gas: Univ. N. Mex. Pub. in Geology, no. 4, 286 pp.

Kelley, V.C. and Thompson, T.B., 1964, Tectonics and geology of the Ruidoso-Carrizozo Region, central New Mexico: in Guidebook of the Ruidoso Country, New Mexico Geol. Soc., pp. 110-121.

King, E.G., Barany, R., Weller, W.W., and Pankratz, L.B., 1967, Thermodynamic properties of forsterite and serpentine: U.S. Bur. Mines Rept. Div. 6962, 19 pp.

Kottlowski, F.E., Flower, R.H., Thompson, M.L., and Foster, R.W., 1956, Stratigraphic studies of the San Andres Mountains, New Mexico: N. Mex. Inst. of Min. and Tech., State Bur. Mines and Min. Res. Mem. 1, 132 pp.

New Mexico Quality Control Commission, 1975, Central closed basins plan: Santa Fe, New Mexico.

Robie, R.A. and Waldbaum, D.R., 1968, Thermodynamic properties of Minerals and related substances at 298.15°K (25°C) and one atmosphere (1.013 bars) pressure and at higher temperatures: U.S. Geol. Survey Bull. 1259, 256 pp.

Schnake, C.J., 1977, A thermodynamic appraisal of contact metamorphism of siliceous dolomitic limestones: unpublished Master's thesis, N. Mex. Inst. of Min. and Tech.

Sheridan, M.J., 1947, Lincoln County iron deposits, New Mexico: U.S. Bur. Mines Rpt. Inv. 3988.

Smith, C.T., 1964, Geology of the Little Black Peak quadrangle, Socorro and Lincoln Counties, New Mexico: in Guidebook of the Ruidoso Country, New Mexico Geol. Soc., pp 92-99.

Smith, C.T., and Budding, A.J., 1959, Reconnaissance geologic map of the Little Black Peak quadrangle, east half, New Mexico: N. Mex. Inst. Min. and Tech., State Bur. Mines and Min. Res. Geol. map 11.

Travis, R.B., 1955, Classification of rocks: Quarterly of the Colorado School of Mines, v. 50, no. 1.

Walker, G.W. and Osterwald, F.W., 1956, Uraniferous magnetite-hematite deposit at the Prince Mine, Lincoln County, New Mexico: Econ. Geol., v. 51, pp. 213-222.

Weber, R.H., 1964, Geology of the Carrizozo quadrangle, New Mexico: in Guidebook of the Ruidoso Country, New Mex. Geol. Soc. pp. 100-110.

Wilpolt, R.H. and Wanek, A.A., 1951, Geology of the region from Socorro and San Antonio east to Chupadera Mesa, Socorro County, New Mexico: U.S. Geol. Survey Oil and Gas Inv. Map OM 121.

This thesis is accepted on behalf of the faculty of the Institute by the following committee:

Richard E. Brans

Marcel W. Bodine, Jr.

A. J. Buddington

Clay T. Smith

Date 8/13/76